

Causal inference with misspecified network interference structure

Bar Weinstein* and Daniel Nevo†

Department of Statistics and Operations Research, Tel Aviv University

March 7, 2024

Abstract

Under interference, the potential outcomes of a unit depend on treatments assigned to other units. A network interference structure is typically assumed to be given and accurate. In this paper, we study the problems resulting from misspecifying these networks. First, we derive bounds on the bias arising from estimating causal effects under a misspecified network. We show that the maximal possible bias depends on the divergence between the assumed network and the true one with respect to the induced exposure probabilities. Then, we propose a novel estimator that leverages multiple networks simultaneously and is unbiased if one of the networks is correct, thus providing robustness to network specification. Additionally, we develop a probabilistic bias analysis that quantifies the impact of a postulated misspecification mechanism on the causal estimates. We illustrate key issues in simulations and demonstrate the utility of the proposed methods in a social network field experiment and a cluster-randomized trial with suspected cross-clusters contamination.

Keywords: Misspecification, SUTVA, spillovers, contamination, probabilistic bias analysis.

*barwein@mail.tau.ac.il

†The authors gratefully acknowledge support from the Israel Science Foundation (ISF grant No. 827/21)

1 Introduction

A common assumption in causal inference is that there is *no interference* (Cox, 1958). However, interference between units is present in many settings, e.g., in studying the effect of preventive measures on the spread of infectious diseases (Halloran and Struchiner, 1995). Removing the no-interference assumption allows for testing the null hypothesis of no treatment effects (Rosenbaum, 2007), but not for unbiased estimation of treatment effects (Basse and Airolidi, 2018). Thus, relaxing the no-interference assumption must be accompanied by an assumed interference structure. There is *partial interference* when the interaction between units is assumed to occur only within well-separated clusters (Hudgens and Halloran, 2008; Tchetgen Tchetgen and VanderWeele, 2012). A more general form of interference is *network interference*, in which relationships between units are represented by edges in a postulated network (Ugander et al., 2013; Aronow and Samii, 2017; Forastiere et al., 2020; Leung, 2020; Tchetgen Tchetgen et al., 2020; Ogburn et al., 2022).

Correctly specifying the network can be challenging due to the complicated interactions between units that often accompany scenarios with interference. One example is Paluck et al. (2016), who conducted a study on the effects of a randomized educational intervention within a social network of students. They derived the network through questionnaires that asked students to list up to ten friends they spend time with. However, if the answers do not accurately reflect actual social interactions or if some students interact with more than ten friends, the network constructed from the questionnaire answers will misrepresent the actual social interactions and lead to a misspecified interference structure. Another example is Hayek et al. (2022), who estimated the indirect protective effect of parental vaccination against children’s SARS-CoV-2 infection. Their model specification assumed that indirect vaccine effects occur only within family households. Since infection between households is possible, the assumed interference structure is also misspecified, as the vaccination status of other community members should affect infection (Halloran and Struchiner, 1991). These examples demonstrate that correctly specifying the network interference structure is a difficult task. Nevertheless, in practice, the interference structure is typically assumed to be given, unique, and correctly specified (e.g., Aronow and Samii, 2017; Forastiere et al., 2020; Ogburn et al., 2022).

In this paper, we extend the exposure mapping framework (Ugander et al., 2013; Aronow and Samii, 2017) to explicitly account for the possibility of a misspecified network interference structure. The latter can be viewed as a type of exposure mapping misspecification. Previous work studied exposure mapping misspecification without explicitly distinguishing between the specification of the map and the network (Aronow and Samii, 2017; Sävje, 2023). We develop a formal framework that highlights that the correctly specified network interference structure might not be unique, i.e., different networks can represent the same effective interference structure and show that uniqueness arises under limitations on the exposure mapping and on the potential outcomes. We consider a randomized experiment

on a network of units and derive bounds on the bias of commonly used estimators when an incorrect interference structure is assumed. Then, we propose solutions for two common scenarios: (1) when researchers have multiple networks but are uncertain which one is correctly specified, and (2) when a single network is readily available but researchers are concerned about deviations from it. For the first scenario, we propose a novel estimator that incorporates multiple networks simultaneously and prove its robustness to network misspecification, that is, the estimator is unbiased if one of the networks correctly specifies the interference structure. We also illustrate that this unbiasedness may come with a price of increased variance, where the magnitude of the increase depends on the number of networks and their relative (dis)similarity. For the second scenario, we develop a probabilistic bias analysis (PBA) (Lash and Fink, 2003; Greenland, 2005) framework that uses an induced probability distribution for the true network given the specified network and examines how deviations from the specified interference structure impact the causal estimates.

The rest of the paper is organized as follows. Section 2 reviews relevant literature on causal inference with interference. Section 3 introduces notations and formalizes the problem by providing assumptions, definitions, and causal estimands. Section 4 lists examples of misspecified networks and shows that commonly used estimators are biased when the network is misspecified. Section 5 presents the novel network-misspecification-robust estimator and develops a PBA framework. Section 6 conducts simulation studies to illustrate the bias from using a misspecified network and the bias-variance tradeoff of the network-misspecification-robust estimator. Section 7 analyzes a social network field experiment and a cluster-randomized trial with the proposed methods. Finally, Section 8 discusses the findings and potential areas for future research.

The R package `MisspecifiedInterference` implementing our methodology is available from https://github.com/barwein/Misspecified_Interference. Simulations and data analyses reproducibility materials of the results are available from <https://github.com/barwein/CI-MIS>. All the proofs and derivations are given in Appendix A.

2 Related literature

Causal estimands under interference can be defined in different ways. One option is to define the effects as contrasts of the average of expected potential outcomes marginalized by the impact of other units' treatment (Hudgens and Halloran, 2008; Tchetgen Tchetgen and VanderWeele, 2012; Sävje et al., 2021; Hu et al., 2022). Another assumes structural causal models (Tchetgen Tchetgen et al., 2020; Ogburn et al., 2022), such as the linear-in-means model (Manski, 1993). In this paper, we build on the exposure mapping approach (Ugander et al., 2013; Aronow and Samii, 2017) which uses exposure values to define causal effects, similar to the summarizing functions assumed in other papers (e.g., Hong and Raudenbush,

2006; Manski, 2013; Forastiere et al., 2020; Leung, 2020; Ogburn et al., 2022).

There are various methods for estimating causal effects under uncertain or partially-measured interference structures. These methods typically either impute missing edges or assume a specific measurement error model. Bhattacharya et al. (2020) used a causal discovery method to estimate causal effects in partial interference settings with unknown within-clusters network structure. Tortú et al. (2021) suggested imputing missing edges with a network model that is first trained on the available edges. When interference between units occurs within both online and offline networks, Egami (2020) proposed a sensitivity analysis that examines the impact of not observing the offline network on the causal estimates. Under the linear-in-means model, Boucher and Houndetoungan (2022) considered estimation when only a distribution of the network is available, and Griffith (2021) illustrated the impact of edge censoring (see Example 2 in Section 4). Building on the exposure mapping framework, Li et al. (2021) considered networks that are measured with random error and constructed unbiased estimators that require assumptions on the measurement error and at least three noisy network measurements. In a similar setting, Hardy et al. (2019) assumed a parametric model for the exposure mapping and suggested an EM algorithm for the estimation of causal effects. In comparison to both Li et al. (2021) and Hardy et al. (2019) which assumed a specific network measurement error model and implicitly regard the true network as unique, our approach acknowledges the possibility that the correct network is not unique and does not view the network specification problem as a measurement error problem, thus it can be viewed as complementary.

When the network interference structure is unavailable, it was recently shown that the total treatment effect, the effect of treating vs. not treating all the units, can be still estimated consistently (Sävje et al., 2021; Cortez et al., 2022; Yu et al., 2022). However, studying more intricate channels of interference requires a network measurement (Yu et al., 2022).

3 Notations, assumptions and causal estimands

3.1 Setup

Consider a population of n units, indexed by $i = 1, \dots, n$. Let \mathbf{Z} be the treatment assignment vector of the entire population and let \mathcal{Z} denote the treatments' space which is assumed to be finite, e.g., for binary treatments $\mathcal{Z} = \{0, 1\}^n$. Each unit has a function $Y_i : \mathcal{Z} \rightarrow \mathbb{R}$ denoting the *potential* or *counterfactual* outcomes (Neyman, 1923), that is, $Y_i(\mathbf{z})$ is the outcome of i when, possibly contrary to the fact, the population treatment is set to $\mathbf{z} \in \mathcal{Z}$. In our framework, $Y_i(\mathbf{z})$ are fixed, hence randomness arises solely from the assignment of \mathbf{Z} .

We focus on network interference that, for simplicity, is assumed to be represented by

an undirected and unweighted network. Extensions to directed and weighted networks are possible with appropriate modifications (see Section 8). The network is a collection of nodes and edges, where each node represents a unit and the edges indicate the interference between units, as we define below. We represent the network by its symmetric adjacency matrix $\mathbf{A} \in \mathbb{R}^{n \times n}$, with $A_{ij} = 1$ only if an edge exists between units i and j , and by convention $A_{ii} = 0$. Let $\mathcal{N}_i(\mathbf{A}) = \{j : A_{ij} = 1\}$ be the set of *neighbors* of unit i . Let \mathcal{A} denote the space of all undirected and unweighted networks of size n . We take the common neighborhood network interference assumption (Forastiere et al., 2020; Ogburn et al., 2022) which states that interference occurs only between neighbors, that is, for any $\mathbf{z}, \mathbf{z}' \in \mathcal{Z}$

$$\text{if } z_i = z'_i \text{ and } z_j = z'_j \ \forall j \in \mathcal{N}_i(\mathbf{A}), \text{ then } Y_i(\mathbf{z}) = Y_i(\mathbf{z}'). \quad (1)$$

For binary treatments, Equation (1) implies that each unit has 2^{d_i+1} potential outcomes, where $d_i = |\mathcal{N}_i(\mathbf{A})|$ is the degree of unit i . It is plausible that some structure can be put on the similarity between the different 2^{d_i+1} potential outcomes thus reducing their effective number. To this end, we assume that the treatments affect the outcomes only through values of an *exposure mapping* (Ugander et al., 2013; Aronow and Samii, 2017). The exposure mapping f is a function that maps from the treatments and networks spaces into $L > 0$ different exposure levels $f : \mathcal{Z} \times \mathcal{A} \rightarrow \mathcal{C} = \{c_1, \dots, c_L\}$. Adapting the neighborhood network interference structure, we assume that for any unit i the values of f depend only on the treatments assigned to its neighbors. Formally, let \mathbf{A}_i be the i -th row of \mathbf{A} . We denote the exposure values by $f(\mathbf{z}, \mathbf{A}_i)$.

Turning to the treatments' assignment, we assume that the experimental design $\Pr(\mathbf{Z} = \mathbf{z})$ is known. Let $\mathbb{I}\{\cdot\}$ denote the indicator function. We define the probability that unit i has exposure value c_ℓ under \mathbf{A} by

$$p_i^{(\mathbf{A})}(c_\ell) := \mathbb{E}_{\mathbf{Z}}[\mathbb{I}\{f(\mathbf{Z}, \mathbf{A}_i) = c_\ell\}] = \sum_{\mathbf{z} \in \mathcal{Z}} \Pr(\mathbf{Z} = \mathbf{z}) \mathbb{I}\{f(\mathbf{z}, \mathbf{A}_i) = c_\ell\}.$$

Calculating $p_i^{(\mathbf{A})}(c_\ell)$ could be computationally intensive due to the large dimension of \mathcal{Z} , but approximating it by re-sampling from $\Pr(\mathbf{Z} = \mathbf{z})$ is possible (see Appendix F). Moving on, we will treat $p_i^{(\mathbf{A})}(c_\ell)$ as given and ignore its estimation error, which can be easily bounded (Aronow and Samii, 2017). The following definition is the exposure mapping analogue of the standard positivity assumption.

Definition 1 (Positivity). We say that $\mathbf{A} \in \mathcal{A}$ satisfies positivity if $p_i^{(\mathbf{A})}(c_\ell) > 0$ for all units $i = 1, \dots, n$ and exposure values $\ell = 1, \dots, L$.

Given the experimental design and the exposure mapping, positivity is a property of the network. There are scenarios when positivity will not hold for some networks. For instance, if f indicates whether a unit is treated and at least one of its neighbors is treated as well (Aronow and Samii, 2017), then if a unit is isolated ($\mathcal{N}_i(\mathbf{A}) = \emptyset$), there will be a structural violation of positivity for some exposure values.

3.2 Correctly specified network

Assume that for each unit there exists a function $\tilde{Y}_i : \mathcal{C} \rightarrow \mathbb{R}$ that maps the exposure values, i.e., $\tilde{Y}_i(c_\ell)$ is the outcome of unit i when its exposure value is c_ℓ . We denote $\tilde{Y}_i(c_1), \dots, \tilde{Y}_i(c_L)$ as the induced potential outcomes expressed in terms of exposure values. To connect \tilde{Y} to the potential outcomes Y , the researcher must specify a network that accurately represents the interference structure, as expressed in the following definition.

Definition 2. (Correctly specified interference structure) For an exposure mapping f , we say that the interference structure is correctly specified by $\mathbf{A} \in \mathcal{A}$, if \mathbf{A} satisfies Definition 1, and for $i = 1, \dots, n$ and all $\mathbf{z} \in \mathcal{Z}$,

$$\text{if } f(\mathbf{z}, \mathbf{A}_i) = c_\ell, \text{ then } Y_i(\mathbf{z}) = \tilde{Y}_i(c_\ell).$$

If some \mathbf{A} satisfies Definition 2, then for all \mathbf{z}, \mathbf{z}' , if $f(\mathbf{z}, \mathbf{A}_i) = f(\mathbf{z}', \mathbf{A}_i)$ then $Y_i(\mathbf{z}) = Y_i(\mathbf{z}')$. The latter property is often called an *exclusion restriction* condition (e.g., Puelz et al., 2022). Therefore, Definition 2 formalizes the role of the exposure mapping as a bridge between the network \mathbf{A} and treatments \mathbf{z} on one side and the potential outcomes on the other side. We assume there exists at least one network that satisfies Definition 2. This implies that we can use $\tilde{Y}_i(c_\ell)$ instead of $Y_i(\mathbf{z})$.

Remark 1. A misspecified interference network can be viewed as a specific case of exposure mapping misspecification. In our framework, we separate the role of the assumed network \mathbf{A} and the mapping $f(\mathbf{z}, \mathbf{A}_i)$. This framework highlights that misspecification of the exposure mapping can result from an incorrect map f or a network \mathbf{A} . Definition 2 implies that the map f is correct but the network \mathbf{A} may not be, which is the focus of this paper. Previous work on misspecified exposure mapping studied the impact of an incorrect mapping without differentiating between the map and the network (Aronow and Samii, 2017; Sävje, 2023).

Typically, it is explicitly or implicitly assumed that a unique network correctly specifies the interference structure (Aronow and Samii, 2017; Hardy et al., 2019; Li et al., 2021). We now formalize that, under the exposure mapping framework, the uniqueness property holds under further assumptions on the exposure mapping and the potential outcomes. The following two assumptions are required only to illustrate the uniqueness of the correct network and are not needed for the theoretical guarantees we provide in subsequent sections.

Assumption 1. For all \mathbf{A}, \mathbf{A}' that satisfy Definition 1, if $\mathbf{A} \neq \mathbf{A}'$, there exists $\mathbf{z} \in \mathcal{Z}$ such that for some i , $f(\mathbf{z}, \mathbf{A}_i) \neq f(\mathbf{z}, \mathbf{A}'_i)$.

Assumption 1 states that for any two different networks, there is a treatment vector that results in two different exposure values for at least one unit. In Appendix A, we show that an extended version of a commonly assumed exposure mapping (Aronow and Samii, 2017),

which we also utilize in this paper, satisfies Assumption 1. The following assumption states that the sharp null hypothesis does not hold.

Assumption 2. $\tilde{Y}_i(c_\ell) \neq \tilde{Y}_i(c_k)$, for all $\ell \neq k = 1, \dots, L$, $i = 1, \dots, n$.

Assumption 2 is strong and is only needed for the following proposition.

Proposition 1. *Assume there exists a network $\mathbf{A}^* \in \mathcal{A}$ that satisfies Definition 2. Then, under Assumptions 1-2, \mathbf{A}^* is unique.*

In the contrapositive, when \mathbf{A}^* is not unique, at least one of Assumptions 1 and 2 does not hold. If Assumption 1 does not hold, there exist at least two different networks under which f maps to identical values for all treatment vectors, making the networks indistinguishable in terms of the exposure values. If Assumption 2 does not hold, then two different networks that yield two different exposure values c_ℓ, c_k , for some z , will result in the same potential outcomes $\tilde{Y}_i(c_\ell) = \tilde{Y}_i(c_k)$ for at least one unit. Both cases highlight that different networks can represent the same interference structure. In what follows, we let \mathbf{A}^* be a network that correctly specifies the interference structure. The network \mathbf{A}^* can be unique or part of an equivalence class of networks that yield tantamount interference structures which we denote by $\mathcal{A}^* \subseteq \mathcal{A}$. That is, \mathcal{A}^* is the set of all networks satisfying Definition 2, and $\mathbf{A}^* \in \mathcal{A}^*$. Note that under the sharp null ($\tilde{Y}_i(c_k) = \tilde{Y}_i(c_\ell)$, $\forall i, k, \ell$), given any exposure value, all other potential outcomes $\tilde{Y}(\cdot)$ are imputable (Athey et al., 2018; Basse et al., 2019; Puelz et al., 2022), thus any network will correctly specify the interference structure.

Remark 2. Under the neighborhood interference assumption (Equation (1)), without the further assumption of exposure mapping, if \mathbf{A} is correctly specified, then any superset of it (i.e., networks with edges that are a superset of \mathbf{A} edges), will by extension be correctly specified as well. In the extreme, the fully connected network is always correctly specified. By construction, the network that correctly specifies the interference will not be unique. Under the exposure mapping assumption, that will no longer hold. Proposition 1, by its contrapositive, implies that a superset of a correctly specified network will also satisfy Definition 2 only under further limitations on the exposure mapping and potential outcomes. Namely, under the exposure mapping framework, the fully connected network is not necessarily correctly specified. Thus, exposure mapping, by its summarizing property, reduces the number of effective potential outcomes but entails a different class \mathcal{A}^* of correctly specified networks.

Turning to the observed data, we denote by $\mathbf{Z}^o = (Z_1^o, \dots, Z_n^o)$ and $\mathbf{Y}^o = (Y_1^o, \dots, Y_n^o)$ the observed treatments and outcomes vector, respectively. We assume that the observed outcomes are related to the potential outcomes in the following manner.

Assumption 3 (Consistency). *The observed outcomes are generated from one of the potential outcomes by*

$$Y_i^o = \sum_{j=1}^L \mathbb{I}\{f(\mathbf{Z}^o, \mathbf{A}_i^*) = c_j\} \tilde{Y}_i(c_j), \quad i = 1, \dots, n,$$

where $\mathbf{A}^* \in \mathcal{A}^*$.

Notice that even if \mathcal{A}^* is not a singleton, all networks in it will result in the same observed outcomes. That is, the sum $\sum_{j=1}^L \mathbb{I}\{f(\mathbf{Z}^o, \mathbf{A}_i^*) = c_j\} \tilde{Y}_i(c_j)$ is equal for any $\mathbf{A}^* \in \mathcal{A}^*$.

3.3 Causal estimands

To define causal effects under the above-described framework, we first define the mean potential outcomes $\mu(c_\ell) = \frac{1}{n} \sum_{i=1}^n \tilde{Y}_i(c_\ell)$, $\ell = 1, \dots, L$. Causal effects are defined as the difference in the mean potential outcomes,

$$\tau(c_\ell, c_k) = \mu(c_\ell) - \mu(c_k). \quad (2)$$

This definition is common in the literature of causal inference in networks (e.g., Ugander et al., 2013; Aronow and Samii, 2017; Forastiere et al., 2020). Such causal effects typically do not correspond to actual feasible interventions, as one cannot individually intervene on the exposure level. For example, it is impossible that all units are untreated and also have at least one treated friend. Nevertheless, the estimands in (2) offer insights into the mechanism of treatment spillover. They elucidate aspects such as the presence and magnitude of indirect effects induced by the treatments, thereby enhancing our understanding of how the propagation of treatments across a network of units influences the outcomes.

4 Bias from using a misspecified network

Let \mathbf{A}^{sp} be the network specified by the researchers. In this section, we study the bias resulting from using a misspecified network, i.e., when $\mathbf{A}^{sp} \notin \mathcal{A}^*$. We first provide conceivable examples for networks that incorrectly specify the interference structure.

Example 1 (Incorrect reporting of social connections). Networks can be created from participant self-reported surveys listing frequently interacted friends (Paluck et al., 2016; Cai et al., 2015) or through epidemiological contact tracing (Nagarajan et al., 2020). However, determining the interference structure through questionnaires and surveys can be susceptible to inaccuracies. For instance, if participants omit friends they interact with or if listed friends are not relevant for interference, the specified network edges may fail to reflect the actual interference structure. A misspecified network due to incorrect reporting of social interactions is illustrated in Figure 1(A).

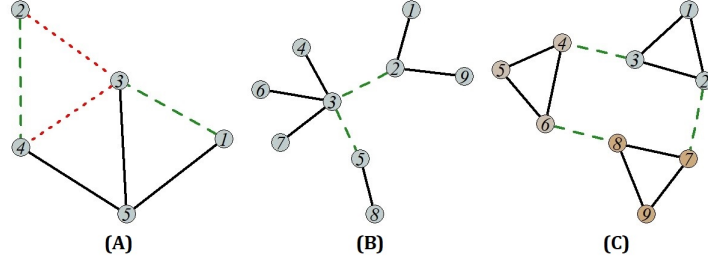


Figure 1: Schematic view of network misspecification. Edges in dashed lines are missing whereas edges in dotted lines are assumed to be present but should be removed. (A) Network with an incorrect list of edges. (B) Network with edges censored at $K = 3$. Node 3 has five edges but two are censored ($2 - 3, 3 - 5$). (C) Cross-clusters contamination with three clusters.

Example 2 (Censoring). Questionnaires often request participants to list their top $K > 0$ friends, but this limitation can result in neglected social connections, known as *censoring* of edges (Griffith, 2021). For example, Cai et al. (2015) and Paluck et al. (2016) asked participants to list five and ten friends, respectively. To assess the extent of censoring present, one can look at the percentage of participants that listed the maximum number of friends, which were 91% in Cai et al. (2015) and 46% in Paluck et al. (2016). An illustration of censoring can be seen in Figure 1(B).

Example 3 (Reciprocity). Undirected network edges are mutual, meaning if participant j treatment interferes with participant i , then participant i also interferes with participant j . When constructing undirected networks from questionnaire data, researchers can assume an edge exists between two participants if one of them listed the other as a friend or, alternatively, if both participants listed each other. These two options will likely result in different network structures. Cai et al. (2015) analyzed the same dataset under both options and found moderate differences.

Example 4 (Temporality). Social interactions between people are constantly changing and evolve over time (Ebel et al., 2002). Derived social networks are often only a “snapshot” of these interactions. Typically, the network is specified from data collected before treatment allocation. However, specifying the network using data from later periods often results in different network structures (e.g., Schaefer et al., 2012; Paluck et al., 2016). Paluck et al. (2016) specified networks from questionnaires in the pre- and post-intervention periods which lasted a year. They estimated that only 42.2% of reported ties in the pre-intervention period persisted in the post-intervention one. Nonetheless, using a network that is measured post-treatment necessitates the assumption that treatment did not affect the network structure and further assumptions required by the dynamic nature of the problem.

Example 5 (Cross-clusters contamination). In partial interference settings, interference is assumed to occur only between units within the same cluster. The resulting network is

composed of well-separated clusters, but contamination can occur between clusters, leading to unaccounted-for interference. For example, Hayek et al. (2022) estimated the indirect effect of vaccination against SARS-CoV-2 while implicitly assuming that the protective effect was limited to households. However, if infection can occur outside the household, then the vaccination status of individuals from different households may affect household members, resulting in contamination between clusters. The network structure of clusters with possible contamination is illustrated in Figure 1(C).

4.1 Estimation bias

Given the specified network \mathbf{A}^{sp} , the mean potential outcomes $\mu(c_\ell)$ are often estimated by the Horvitz-Thompson (HT) estimator (Ugander et al., 2013; Aronow and Samii, 2017)

$$\hat{\mu}_{\mathbf{A}^{sp}}(c_\ell) = \frac{1}{n} \sum_{i=1}^n \frac{\mathbb{I}\{f(\mathbf{Z}^o, \mathbf{A}_i^{sp}) = c_\ell\}}{p_i^{(\mathbf{A}^{sp})}(c_\ell)} Y_i^o. \quad (3)$$

Let $\tilde{n}(\mathbf{A}, c_\ell) := \sum_{i=1}^n \frac{\mathbb{I}\{f(\mathbf{Z}^o, \mathbf{A}_i) = c_\ell\}}{p_i^{(\mathbf{A})}(c_\ell)}$. Alternatively, the Hajek estimator,

$$\hat{\mu}_{\mathbf{A}^{sp}}^H(c_\ell) = \frac{1}{\tilde{n}(\mathbf{A}^{sp}, c_\ell)} \sum_{i=1}^n \frac{\mathbb{I}\{f(\mathbf{Z}^o, \mathbf{A}_i^{sp}) = c_\ell\}}{p_i^{(\mathbf{A}^{sp})}(c_\ell)} Y_i^o, \quad (4)$$

was shown to have a better finite-sample accuracy (Särndal et al., 2003). Subsequently, $\tau(c_\ell, c_k)$ is estimated by the plug-in HT estimator $\hat{\tau}_{\mathbf{A}^{sp}}(c_\ell, c_k) = \hat{\mu}_{\mathbf{A}^{sp}}(c_\ell) - \hat{\mu}_{\mathbf{A}^{sp}}(c_k)$, and similarly for the Hajek estimator $\hat{\tau}_{\mathbf{A}^{sp}}^H$.

The researcher estimates the causal effects with \mathbf{A}^{sp} , which, as previously indicated, may or may not be in \mathcal{A}^* , i.e., \mathbf{A}^{sp} might fail to correctly represent the interference structure. By replacing Y_i^o in (3) with its definition under consistency (Assumption 3), we can write the HT estimator as

$$\hat{\mu}_{\mathbf{A}^{sp}}(c_\ell) = \frac{1}{n} \sum_{i=1}^n \underbrace{\left[\frac{\mathbb{I}\{f(\mathbf{Z}^o, \mathbf{A}_i^{sp}) = c_\ell\}}{p_i^{(\mathbf{A}^{sp})}(c_\ell)} \right]}_{\text{Selection and weighting}} \underbrace{\sum_{j=1}^L \mathbb{I}\{f(\mathbf{Z}^o, \mathbf{A}_i^*) = c_j\} \tilde{Y}_i(c_j)}_{\text{Observation}}, \quad (5)$$

where \mathbf{A}^* is some network in \mathcal{A}^* (Section 3). Equation (5) clarifies that the selection and weighting of units are performed with \mathbf{A}^{sp} , whereas the observed outcomes are generated by \mathcal{A}^* . Thus, if $\mathbf{A}^{sp} \notin \mathcal{A}^*$, estimation using a misspecified network \mathbf{A}^{sp} could yield erroneous results due to selecting the wrong units or weighing the observed outcomes with possibly wrong weights. We now provide a formal result to reflect this intuition. Assume that the potential outcomes are bounded.

Assumption 4 (Bounded potential outcomes). *There exists a constant $\kappa > 0$ such that $|\tilde{Y}_i(c_\ell)| \leq \kappa$, $\forall i, \ell$.*

For exposure values c_ℓ, c_k and networks \mathbf{A}, \mathbf{A}' , define the joint probability that unit i is exposed to c_ℓ under \mathbf{A} and to c_k under \mathbf{A}' by

$$p_i^{(\mathbf{A}, \mathbf{A}')} (c_\ell, c_k) = \mathbb{E}_{\mathbf{Z}} \left[\mathbb{I} \left\{ \{f(\mathbf{Z}, \mathbf{A}_i) = c_\ell\} \cap \{f(\mathbf{Z}, \mathbf{A}'_i) = c_k\} \right\} \right]. \quad (6)$$

The following theorem derives bounds on the absolute bias of the HT estimator $\hat{\mu}_{\mathbf{A}^{sp}}$, and shows that, given the exposure mapping, the bounds depend on the divergence of \mathbf{A}^{sp} from networks in \mathcal{A}^* (in terms of exposure mapping) and on the range of the potential outcomes.

Theorem 1. *Let \mathbf{A}^* be an arbitrarily chosen network from \mathcal{A}^* , and let $\mathbf{A}^{sp} \in \mathcal{A}$ be a network satisfying Definition 1. Under Assumptions 3-4, for any c_ℓ ,*

$$\left| \mathbb{E}_{\mathbf{Z}} [\hat{\mu}_{\mathbf{A}^{sp}}(c_\ell)] - \mu(c_\ell) \right| \leq \frac{2\kappa}{n} \sum_{i=1}^n \left[1 - p_i(c_\ell; \mathbf{A}^* \mid c_\ell; \mathbf{A}^{sp}) \right],$$

where $p_i(c_\ell; \mathbf{A}^* \mid c_\ell; \mathbf{A}^{sp}) = \frac{p_i^{(\mathbf{A}^*, \mathbf{A}^{sp})}(c_\ell, c_\ell)}{p_i^{(\mathbf{A}^{sp})}(c_\ell)}$ is the conditional probability that unit i is exposed to c_ℓ under \mathbf{A}^* given it is exposed to c_ℓ under \mathbf{A}^{sp} .

Theorem 1 shows that the bounds on the absolute bias of $\hat{\mu}_{\mathbf{A}^{sp}}$ increases with the divergence of \mathbf{A}^{sp} from \mathbf{A}^* , in terms of resulting exposure levels. Namely, the conditional probabilities $p_i(c_\ell; \mathbf{A}^* \mid c_\ell; \mathbf{A}^{sp})$ quantifies how the extent of misspecification of \mathbf{A}^{sp} impacts the maximal bias. The difference between \mathbf{A}^{sp} and \mathbf{A}^* affects the bias only through their disagreement on the set of exposures. The absolute bias also increases with κ , the assumed bound of the potential outcomes. The maximal bias of the plug-in causal effects estimator $\hat{\tau}_{\mathbf{A}^{sp}}$ follows from Theorem 1 and is given in Appendix A.

We also derive the exact bias of $\hat{\mu}_{\mathbf{A}^{sp}}$ and $\hat{\tau}_{\mathbf{A}^{sp}}$, which are found to be linear combinations of all potential outcomes with weights relating to the conditional probabilities $p_i(c_\ell; \mathbf{A}^* \mid c_k; \mathbf{A}^{sp})$ (Appendix A). Related results were obtained by Hardy et al. (2019) and Li et al. (2021) who derived the bias from using an incorrect network for a specific choice of exposure mapping while assuming \mathbf{A}^* is unique. The following corollary states that the bias is zero when $\mathbf{A}^{sp} \in \mathcal{A}^*$.

Corollary 1. *Under the conditions stated in Theorem 1, if $\mathbf{A}^{sp} \in \mathcal{A}^*$, $\mathbb{E}_{\mathbf{Z}} [\hat{\mu}_{\mathbf{A}^{sp}}(c_\ell)] = \mu(c_\ell)$, $\forall c_\ell$.*

The corollary follows from the fact that if $\mathbf{A}^{sp} \in \mathcal{A}^*$, then in Theorem 1 we can choose $\mathbf{A}^* = \mathbf{A}^{sp}$. Thus, the conditional probabilities are all equal to one, and the bound is equal to zero. Ugander et al. (2013) and Aronow and Samii (2017) proved a similar version of Corollary 1 without considering the class \mathcal{A}^* nor the absolute bias bounds shown in Theorem 1. Regarding the Hajek estimator (4), being a ratio estimator, it is biased even if $\mathbf{A}^{sp} \in \mathcal{A}^*$, but the bias can be bounded as we show in Appendix B.

As mentioned before, in the specific case of the sharp null, $\tilde{Y}_i(c_k) = \tilde{Y}_i(c_\ell)$ ($\forall i, k, \ell$), the interference structure is correctly specified by any network that satisfies positivity. Thus,

Corollary 1 implies that any network structure with a non-zero probability of exposures will yield an unbiased estimation.

5 Dealing with misspecified interference structure

As established in the previous section, a misspecified network may lead to biased estimation. To address this bias, we suggest solutions for two common scenarios. In the first scenario, the researchers have a collection of possible networks but are unsure which is the correct one. Section 5.1 presents an estimator that simultaneously incorporates multiple networks and is unbiased if one of them is correctly specified. In the second scenario, the researchers have a single network but suspect it might be misspecified. For this scenario, Section 5.2 introduces a PBA framework that quantifies the impact of systematic error in \mathbf{A}^{sp} on the causal estimates. Practical guidelines are given in Section 5.3.

5.1 Network-misspecification-robust estimator

Assume that a researcher has a collection \mathcal{A} of M possible networks but is uncertain which of the networks in \mathcal{A} , if any, correctly specify the interference structure. Typically, \mathcal{A} includes networks that are natural to consider (e.g., different encoding of questionnaire answers). Define

$$I_i^{(\mathcal{A})}(\mathbf{Z}, c_\ell) = \prod_{\mathbf{A} \in \mathcal{A}} \mathbb{I}\{f(\mathbf{Z}, \mathbf{A}_i) = c_\ell\}$$

to be the indicator that equals to one only if the exposure value equals to c_ℓ under each of the networks in \mathcal{A} . Extending the joint probability (6), we define the joint probability that unit i has exposure value c_ℓ under *all* $\mathbf{A} \in \mathcal{A}$ by

$$p_i^{(\mathcal{A})}(c_\ell) = \mathbb{E}_{\mathbf{Z}} \left[I_i^{(\mathcal{A})}(\mathbf{Z}, c_\ell) \right].$$

Our proposed modified HT estimator of $\mu(c_\ell)$ that simultaneously utilizes the M different networks is

$$\hat{\mu}_{\mathcal{A}}(c_\ell) = \frac{1}{n} \sum_{i=1}^n \frac{I_i^{(\mathcal{A})}(\mathbf{Z}^o, c_\ell)}{p_i^{(\mathcal{A})}(c_\ell)} Y_i^o. \quad (7)$$

That is, $\hat{\mu}_{\mathcal{A}}(c_\ell)$ selects only units that has exposure value c_ℓ under *all the networks in* \mathcal{A} and weights them with the inverse of the joint probability $p_i^{(\mathcal{A})}(c_\ell)$. The modified estimator of the causal effects $\tau(c_k, c_\ell)$ is the plug-in estimator $\hat{\tau}_{\mathcal{A}}(c_\ell, c_k) = \hat{\mu}_{\mathcal{A}}(c_\ell) - \hat{\mu}_{\mathcal{A}}(c_k)$. As we now show, $\hat{\mu}_{\mathcal{A}}$ is an unbiased estimator of μ if at least one of the networks in \mathcal{A} correctly specifies the interference structure.

Theorem 2. Let \mathcal{A} be a collection of M networks such that each of the networks satisfies Definition 1. Under Assumption 3, if $\mathcal{A} \cap \mathcal{A}^* \neq \emptyset$, then

$$\mathbb{E}_{\mathbf{Z}} \left[\hat{\mu}_{\mathcal{A}}(c_{\ell}) \right] = \mu(c_{\ell}), \quad \forall c_{\ell}.$$

The key property of the estimator $\hat{\mu}_{\mathcal{A}}$ is that by selecting only units with the same exposure values under each of the networks in \mathcal{A} , we are guaranteed to observe the correct exposure value if one of the networks is correctly specified, but agnostic to which network it is. Therefore, we term $\hat{\mu}_{\mathcal{A}}$ a *network misspecification robust* (NMR) estimator. Accordingly, the plug-in estimator $\hat{\tau}_{\mathcal{A}}(c_{\ell}, c_k)$ is unbiased estimator of $\tau(c_{\ell}, c_k)$ if at least one network in \mathcal{A} is correctly specified. Similarly to $\hat{\mu}_{\mathcal{A}}$, we also propose the NMR Hajek estimator

$$\hat{\mu}_{\mathcal{A}}^H(c_{\ell}) = \frac{1}{\tilde{n}(\mathcal{A}, c_{\ell})} \sum_{i=1}^n \frac{I_i^{(\mathcal{A})}(\mathbf{Z}^o, c_{\ell})}{p_i^{(\mathcal{A})}(c_{\ell})} Y_i^o, \quad (8)$$

where $\tilde{n}(\mathcal{A}, c_{\ell}) := \sum_{i=1}^n \frac{I_i^{(\mathcal{A})}(\mathbf{Z}^o, c_{\ell})}{p_i^{(\mathcal{A})}(c_{\ell})}$. Note that $\hat{\mu}_{\mathcal{A}}^H$ selects the same subset of units as $\hat{\mu}_{\mathcal{A}}$, but is biased since it is a ratio estimator (Särndal et al., 2003). In Appendix B, we derive bounds on this bias. In the simulation study (Section 6.1), we found that HT and Hajek NMR estimators had a similar finite-sample bias.

The NMR estimators offer greater flexibility in the network selection as they allow simultaneously taking any combination of networks. However, this flexibility poses a *bias-variance tradeoff*. Using more networks (large M) can remove the bias (if a correct network is included), but it also increases variance due to the reduction in the number of units used and the decreased joint probabilities $p_i^{(\mathcal{A})}$ values. The increase in the variance depends on the number of networks and their relative (dis)similarity with respect to the mapped exposure levels. That is, even if two networks have a different edge set, the number of excluded units by $I_i^{(\mathcal{A})}(\mathbf{Z}^o, c_{\ell})$ will be small if the two different networks result in similar exposure levels for nearly all units. Section 6.2 illustrates this bias-variance tradeoff via a simulation study. We discuss the option of interpolating an NMR estimator and single-network estimators in Section 8.

In Section 5.3 we discuss how the NMR can be applied in practice in the previously discussed examples, and in Section 7.1, we apply the NMR estimator to a social network field experiment in which four different networks are available.

Building on previous work (Aronow and Samii, 2013) based on Young’s inequality, we derive a conservative variance estimator $\widehat{Var}(\hat{\tau}_{\mathcal{A}})$, i.e., its expected value is not smaller than $Var_{\mathbf{Z}}(\hat{\tau}_{\mathcal{A}})$. Variance estimation of Hajek NMR is similarly obtained with Taylor linearization. Full details are provided in Appendix C. In Appendix F, we demonstrate in simulations the conservativeness property.

5.2 Probabilistic bias analysis

When researchers doubt whether the specified network \mathbf{A}^{sp} correctly represents the interference structure (Definition 2), investigating the impact of such misspecification on the causal estimates is of great interest. As discussed in Section 4 and shown in the bias bounds given in Theorem 1, the bias arises due to dissimilarities between \mathbf{A}^{sp} and \mathbf{A}^* .

We propose a PBA framework, which is also known as Monte-Carlo sensitivity analysis. PBA is a general and flexible procedure that yields a quantitative assessment of the impact of a possible *systematic error* on the causal estimates (Lash and Fink, 2003; Greenland, 2005; Fox et al., 2021). PBA was previously applied to various types of systematic errors such as unmeasured confounding, misclassification, and missing data due to non-response (Fox et al., 2021). In our case, the systematic error of interest is network misspecification.

PBA is performed by positing a distribution of bias parameters and calculating via Monte-Carlo simulations the distribution of the bias-corrected estimates. Traditional sensitivity analyses typically focus on a fixed grid of bias parameter values or a parameter value that results in null effects (Rosenbaum, 2002). PBA extends such procedures by postulating a distribution on the bias parameters. The choice of distribution can be non-informative or informative, depending on the application. PBA provides researchers with causal estimates that could account for both systematic error (e.g., unmeasured confounding) and random error (Greenland, 2005). We first focus on the systematic error and then describe how to extend the procedure to account for the random error arising from the random treatment assignment.

Our proposal builds on the idea that \mathbf{A}^* is a perturbed version of \mathbf{A}^{sp} , and the deviation can be represented by a probability distribution. Assume that researchers are uncertain whether \mathbf{A}^{sp} is correctly specified and are concerned that it deviates from \mathbf{A}^* in a certain way. Let $q(\cdot|\cdot)$ denote a generic notation for a conditional probability distribution. The researchers can represent the suspected deviations from \mathbf{A}^{sp} by a probability distribution $q(\mathbf{A}^*|\mathbf{A}^{sp}, \boldsymbol{\theta})$ for some parameter $\boldsymbol{\theta}$. This distribution is the perceived conditional distribution of \mathbf{A}^* given the specified network \mathbf{A}^{sp} . If the correct network \mathbf{A}^* is unknown but suspected to be a deviation from \mathbf{A}^{sp} as encompassed in $q(\mathbf{A}^*|\mathbf{A}^{sp}, \boldsymbol{\theta})$, then it is taken to be a random network that is generated by perturbing \mathbf{A}^{sp} . Reasoning about the network deviation distribution requires researchers to assess how the specified network \mathbf{A}^{sp} diverges from the true network \mathbf{A}^* . In many applications, it is arguably easier than postulating a full data-generating process for \mathbf{A}^* (e.g., as proposed by Boucher and Houndetoungan, 2022) which requires a detailed understanding of the social interactions of interest. For example, if $\theta_t = \Pr(A_{ij}^* = 1 | A_{ij}^{sp} = t)$, $t = 0, 1$, then $q(\mathbf{A}^*|\mathbf{A}^{sp}, \boldsymbol{\theta}) = \prod_{i < j} \sum_{t=0,1} \mathbb{I}\{A_{ij}^{sp} = t\} \theta_t^{A_{ij}^*} (1 - \theta_t)^{1 - A_{ij}^*}$ is an induced distribution that independently removes each of the edges in \mathbf{A}^{sp} with probability $1 - \theta_1$ and adds an edge that is not present in \mathbf{A}^{sp} with probability θ_0 (per edge). Alternatively, it is also possible to take $\Pr(A_{ij}^* = 1 | A_{ij}^{sp} = t) = \theta_t(\mathbf{x}_i, \mathbf{x}_j)$ for covariates \mathbf{x}_i thus allowing for data-based heterogene-

ity, as we discuss in the examples below. The network deviation distribution $q(\mathbf{A}^*|\mathbf{A}^{sp}, \boldsymbol{\theta})$ is coupled with a distribution $q(\boldsymbol{\theta})$ on $\boldsymbol{\theta}$. Together, the postulated bias distribution is $q(\mathbf{A}^*, \boldsymbol{\theta}|\mathbf{A}^{sp}) = q(\mathbf{A}^*|\mathbf{A}^{sp}, \boldsymbol{\theta})q(\boldsymbol{\theta})$.

Given the observed data $(\mathbf{Y}^o, \mathbf{Z}^o, \mathbf{A}^{sp})$, network deviation distribution $q(\mathbf{A}^*|\mathbf{A}^{sp}, \boldsymbol{\theta})$, and $q(\boldsymbol{\theta})$, the PBA proceeds by repeating the following steps multiple times.

- (i) Sample $\boldsymbol{\theta} \sim q(\boldsymbol{\theta})$.
- (ii) Sample $\mathbf{A}^* \sim q(\mathbf{A}^*|\mathbf{A}^{sp}, \boldsymbol{\theta})$.
- (iii) Calculate $\hat{\tau}_{\mathbf{A}^*}(c_\ell, c_k)$, $\ell, k = 1, \dots, L$.

In Step (iii), the HT estimator can be replaced with the Hajek ratio estimator. The above PBA procedure results in a vector of estimates that represents the distribution of the causal estimates under the postulated misspecification mechanism. However, this procedure accounts only for systematic error, i.e., network misspecification as captured by $q(\mathbf{A}^*|\mathbf{A}^{sp}, \boldsymbol{\theta})$. Additional uncertainty arises from *random error*, namely, the treatment allocation distribution. For this reason, Greenland (2005) advocated the incorporation of random error into the PBA. Following Greenland (2005), this could be done by redrawing a causal estimate from $N(\hat{\tau}_{\mathbf{A}^*}, \widehat{Var}(\hat{\tau}_{\mathbf{A}^*}))$ after step (iii), where the normal approximation is justified by Proposition 6.2 of Aronow and Samii (2017). A conservative variance estimator $\widehat{Var}(\hat{\tau}_{\mathbf{A}^*})$ is provided in Appendix C.

PBA can be viewed as approximate Bayesian (Greenland, 2005; MacLehose and Gustafson, 2012). PBA is only approximate Bayesian since the bias distributions $q(\mathbf{A}^*|\mathbf{A}^{sp}, \boldsymbol{\theta})q(\boldsymbol{\theta})$ are not updated with the observed data (MacLehose and Gustafson, 2012). Consequently, researchers can report percentiles of the resulting estimates from the PBA which will serve as approximate credible intervals.

In the specific case where $q(\boldsymbol{\theta})$ is a point-mass at $\boldsymbol{\theta} = \boldsymbol{\theta}^\dagger$, PBA can be repeated for an increasing range of $\boldsymbol{\theta}$ values. In that case, PBA still provides distributions of the estimates, for a grid of increasing $\boldsymbol{\theta}$ values. Thus, PBA can yield conclusions similar to those obtained through a traditional sensitivity analysis. See Appendix F for an illustration of PBA with point-mass $q(\boldsymbol{\theta})$.

To illustrate the practical utility of the proposed PBA, consider again the previously mentioned examples.

Example 1 (cont.). Studying the impact of misspecification resulting from incorrect reporting of social connections can be accomplished by postulating that a proportion of edges are missing or superfluous. For example, as previously discussed, the researchers can take $q(\mathbf{A}^*|\mathbf{A}^{sp}, \boldsymbol{\theta}) = \prod_{i < j} \sum_{t=0,1} \mathbb{I}\{A_{ij}^{sp} = t\} \theta_t^{A_{ij}^*} (1 - \theta_t)^{1-A_{ij}^*}$ where $\theta_t = \Pr(A_{ij}^* = 1 | A_{ij}^{sp} = t)$.

Example 2 (cont.). If units are asked to list their top $K > 0$ friends, then censoring of

edges is a concern. In this case, it is possible to take

$$q(\mathbf{A}^*|\mathbf{A}^{sp}, \boldsymbol{\theta}) = \prod_{i < j} \mathbb{I}\{A_{ij}^{sp} = 0\} \mathbb{I}\{d_i = K \cup d_j = K\} \theta_0^{A_{ij}^*} (1 - \theta_0)^{1 - A_{ij}^*} + \mathbb{I}\{A_{ij}^{sp} = 1\},$$

where d_i is the degree of unit i under \mathbf{A}^{sp} , i.e., randomly add edges between units with probability θ_0 if at least one of the units has a capped degree.

Example 5 (cont.). Studying the impact of cross-clusters contamination can be performed by assuming that edges between units in different clusters occur randomly with probability θ_0 and letting $q(\mathbf{A}^*|\mathbf{A}^{sp}, \boldsymbol{\theta})$ be the product of such probabilities, similarly to the censoring example above. Covariates can also be included. For example, by postulating that the probability of cross-clusters contamination is inversely related to the spatial distance between clusters, the researchers can take $\Pr(A_{ij}^* = 1 | A_{ij}^{sp} = 0) \propto \psi(\mathbf{x}_i, \mathbf{x}_j)$ for a spatial measure \mathbf{x} and some distance function ψ .

In Section 7.2 we apply the PBA for a cluster-randomized trial (CRT) (Venturo-Conerly et al., 2022) in which cross-clusters contamination is suspected. In the analysis, we demonstrate how the PBA can assist in quantifying the impact of various assumptions regarding the systematic error resulting from specifying a partial interference network.

5.3 Practical considerations

The proposed NMR estimator and the PBA are viable remedies for dealing with network misspecification in two common scenarios. Multiple candidate networks are available in the first scenario, whereas, in the second scenario, no additional networks are needed.

Encoding available social information into an interference network involves making additional assumptions and choices. For instance, when social information is gathered from surveys or questionnaires, assumptions regarding reciprocity (Example 3), which questions to use (Example 1), and at what time point (Example 4) will result in multiple networks, each entailing a different set of assumptions. In addition, social information can be available from various sources, e.g., surveys, geospatial data, and online information. In that case, each source of information will yield a different interference network. Thus, when researchers can obtain multiple networks by making disjoint choices or from different sources of information, we recommend using the NMR estimator (Section 5.1) that combines the information from all the derived interference networks simultaneously. Due to the bias-variance tradeoff, only networks deemed relevant should be included.

In other settings, no additional social information can be found and only one interference network is available. Nevertheless, the researchers often justifiably suspect that the specified network is incorrect. For instance, if the network is derived from limited surveys that lead to error (Example 1) or censoring of the edges (Example 2). Another case is when strong assumptions regarding the interference structure seem implausible, e.g., contamina-

tion in partial interference settings (Example 5). In those cases, researchers can postulate the relevant suspected deviations and evaluate their impact on the causal estimates with the proposed PBA (Section 5.2). Note that results from the PBA will depend on the distributions $q(\mathbf{A}^*|\mathbf{A}^{sp}, \boldsymbol{\theta})$ and $q(\boldsymbol{\theta})$. Therefore, we recommend repeating the PBA with different choices for $q(\mathbf{A}^*|\mathbf{A}^{sp}, \boldsymbol{\theta})$ and $q(\boldsymbol{\theta})$ to evaluate the sensitivity of the results. Examining the robustness of the causal estimates to various bias distributions is the key benefit of the PBA.

6 Simulations

We performed a simulation study consisting of two parts. Section 6.1 illustrates the bias resulting from using a misspecified network. Section 6.2 shows the bias-variance tradeoff of the NMR estimators in practice.

For all simulations, the exposure mapping was defined as follows. For network \mathbf{A} and binary treatment vector \mathbf{z} , denote the proportion of treated neighbors of unit i by $g(\mathbf{z}, \mathbf{A}_i) = |\mathcal{N}_i(\mathbf{A})|^{-1} \sum_{j=1}^n A_{ij}z_j$. The heterogeneous thresholds exposure mapping is defined by

$$f(\mathbf{z}, \mathbf{A}_i) = \begin{cases} c_{11}, & z_i \cdot \mathbb{I}\{g(\mathbf{z}, \mathbf{A}_i) > \nu_i\} = 1 \\ c_{01}, & (1 - z_i) \cdot \mathbb{I}\{g(\mathbf{z}, \mathbf{A}_i) > \nu_i\} = 1 \\ c_{10}, & z_i \cdot (1 - \mathbb{I}\{g(\mathbf{z}, \mathbf{A}_i) > \nu_i\}) = 1 \\ c_{00}, & (1 - z_i) \cdot (1 - \mathbb{I}\{g(\mathbf{z}, \mathbf{A}_i) > \nu_i\}) = 1, \end{cases} \quad (9)$$

where $\nu_i \in [0, 1)$ is a known, possibly unit-specific, threshold. The exposure mapping (9) implies the exposure is a result of two components: whether unit i is treated, and whether the proportion of its treated neighbors surpassed the threshold ν_i . If it is further assumed that $\nu_i = 0 \forall i$, (9) reduces to a commonly used exposure mapping (Aronow and Samii, 2017). We generated the potential outcomes by taking $\tilde{Y}_i(c_{00}) \sim U[0.5, 1.5]$ and $\tilde{Y}_i(c_{11}) = \tilde{Y}_i(c_{00}) + 1$, $\tilde{Y}_i(c_{10}) = \tilde{Y}_i(c_{00}) + 0.5$, $\tilde{Y}_i(c_{01}) = \tilde{Y}_i(c_{00}) + 0.25$. Thresholds were sampled from $\nu_i \sim U[0, 1]$ and are assumed to be known. Treatment assignment mechanisms varied between the different scenarios; details are given below. All simulations were repeated for 1000 iterations in each setup. We present and discuss our main findings here. Additional details, specifications, results, and a study focused on the proposed conservative variance estimators are all provided in Appendix F.

6.1 Illustrations of the estimation bias

We considered three scenarios of network misspecification: incorrect reporting of social connections (Example 1); censoring (Example 2); and cross-clusters contamination (Example 5). In the first two scenarios, we examined how estimating the causal effects using misspecified networks biases the results. For the contamination scenario, we studied the

bias resulting from naively assuming the structure of well-separated clusters (i.e., partial interference) when cross-clusters contamination is present.

Scenario (I) (Incorrect reporting of social connections). A single true network \mathbf{A}^* was sampled from a preferential attachment (PA) random network (Barabási and Albert, 1999) with $n = 3000$ nodes. We created several misspecified networks $\tilde{\mathbf{A}}$ by independently adding and removing edges from \mathbf{A}^* with probability $\eta_{1-t,t} = \Pr(\tilde{A}_{ij} = 1 - t | A_{ij}^* = t)$, $t = 0, 1$, for $i \neq j$. We took $\eta := \eta_{0,1}$, fixed $\eta_{1,0} = \eta/100$, and repeated the simulations for $\eta \in \{0.025, 0.05, \dots, 0.25\}$. Treatments were assigned with Bernoulli allocation $\Pr(\mathbf{Z} = \mathbf{z}) = 0.5^n$. For each η value we generated one misspecified network and used it for the estimation of causal effects.

Scenario (II) (Censoring). For the same \mathbf{A}^* as in Scenario (I), the censoring of edges in \mathbf{A}^* was obtained by randomly removing edges of units with more than K edges to obtain a maximum degree of $K \in \{1, \dots, 7\}$. Treatments were assigned with Bernoulli allocation. For each K value, one censored network was created and used in the estimation.

Scenario (III) (Cross-clusters contamination). We illustrate the impact of contamination in spatial settings. We sampled V clusters uniformly on the unit cube $[0, 1]^2$ such that each cluster is fully connected. Let \mathbf{A}^C denote the resulting network. Let $d(v, v') = \|v_c - v'_c\|_1$ be the spatial L_1 distance between clusters v and v' with v_c being the coordinates of cluster v . We generated contamination by letting two units in clusters $v \neq v'$ form an edge independently with probability $p_{v,v'}(\gamma) = \exp\left(-\frac{d(v,v')}{\gamma \bar{D}}\right)$, where $p_{v,v'}(0) = \mathbb{I}\{v = v'\}$ and where $\bar{D} = \binom{V}{2}^{-1} \sum_{v \neq v'} d(v, v')$ is the mean of pairwise clusters distances and $\gamma \geq 0$ controls the magnitude. Thus, $p_{v,v'}$ decays as the distance between clusters increases. For each $\gamma \in \{0.005, 0.01, \dots, 0.05\}$ value we created one contaminated network \mathbf{A}^* , according to which the potential outcomes were generated. We studied how wrongly assuming no contamination (\mathbf{A}^C) biases the estimation of the overall treatment effect $\tau(c_{11}, c_{00})$ (For estimands in CRT see Appendix D). Clusters were independently assigned to treatment with probability 0.5. We repeated the simulation for $V = 500$ clusters of 20 units each (fixed sizes), and $V = 2000$ clusters with sizes between 3 and 7 (varied sizes).

Figure 2 displays the absolute bias in each of the three scenarios. For Scenarios (I) and (II), we report the results for the HT (3) and Hajek (4) estimators of the overall $\tau(c_{11}, c_{00})$ and direct $\tau(c_{10}, c_{00})$ effects, respectively. In Scenario (I), the magnitude of misspecification was controlled by η . When $\eta = 0$, the true network was used, and, as expected from Corollary 1, the bias was practically zero. As one might expect, the absolute bias increased with η . In Scenario (II), as the censoring threshold K decreased, the censoring increased, and accordingly so was the bias. Turning to Scenario (III), when there was

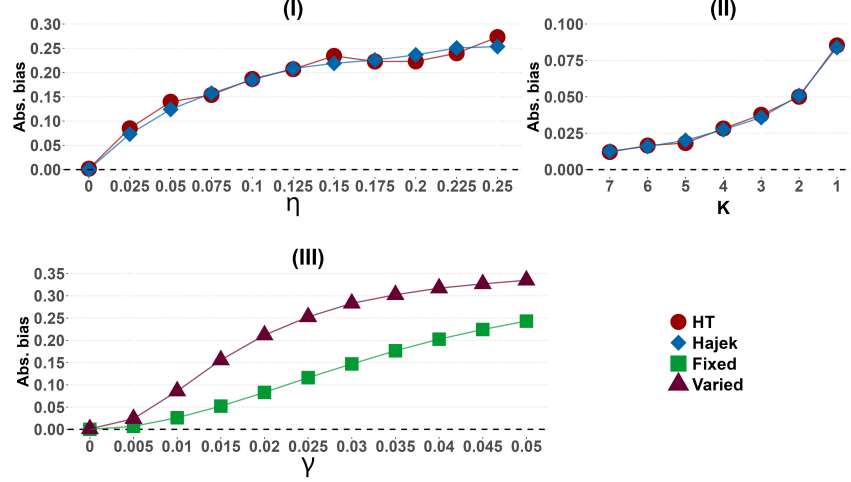


Figure 2: Absolute bias ($|Ave(\hat{\tau}) - \tau|$) due to misspecified network. In Scenarios (I) and (II), $\tau(c_{11}, c_{00})$ and $\tau(c_{10}, c_{00})$, respectively, were estimated with both HT (circles) and Hajek (diamonds) estimators. In Scenario (I), η controls the misspecification level. In Scenario (II), K is the censoring threshold. Scenario (III) shows how contamination level γ impacts the bias of $\tau(c_{11}, c_{00})$ in a CRT with fixed (squares) and varied (triangles) clusters size. True causal effects are $\tau(c_{10}, c_{00}) = 0.5, \tau(c_{11}, c_{00}) = 1$.

no contamination ($\gamma = 0$) the bias in estimating $\tau(c_{11}, c_{00})$ was practically zero, and as contamination increased the bias grew as well. In both Scenarios (I) and (II), the absolute bias of the indirect effects (e.g., $\tau(c_{01}, c_{00})$) was larger than that of the direct effects (e.g., $\tau(c_{10}, c_{00})$) (Appendix F). These results can be intuitively explained by recognizing that, under the exposure mapping (9), network misspecification may lead us to classify a person with true exposure level c_{j0} to exposure level c_{j1} (and vice versa), but will not affect j (for either $j = 0$ or $j = 1$). The estimated Monte-Carlo bias shown here was found to be almost identical to the analytic bias, as derived in Appendix A. Details are given in Appendix F.

6.2 Bias-variance tradeoff of the NMR estimators

The second simulation study illustrates the bias-variance tradeoff of the NMR estimators. Taking the true network \mathbf{A}^* to be the same as in Scenarios (I) and (II) of Section 6.1, we generated from \mathbf{A}^* five misspecified networks $\mathbf{A}^a, \dots, \mathbf{A}^e$ by independently adding and removing edges using $\eta_{0,1} = 0.25$ and $\eta_{1,0} = \eta_{0,1}/100$ with $\eta_{1-t,t}$ as defined in Section 6.1. In total, there were six available networks. After assigning treatments with Bernoulli allocation, we calculated the NMR estimators under each of the $\binom{6}{M}$ possible combinations of \mathcal{A} specifications for each $M = 1, \dots, 6$. For example, if $M = 2$, these possible \mathcal{A} combinations are $\left\{ \{\mathbf{A}^*, \mathbf{A}^a\}, \{\mathbf{A}^*, \mathbf{A}^b\}, \dots, \{\mathbf{A}^d, \mathbf{A}^e\} \right\}$.

Figure 3 shows the absolute bias, standard deviation (SD), and root-mean-squared-error (RMSE) of the Hajek NMR estimator for the indirect effect $\tau(c_{11}, c_{10})$. The bias was practically zero whenever $\mathbf{A}^* \in \mathcal{A}$, and larger than zero when it was not the case. The SD increased with M , regardless if \mathbf{A}^* was included or not, due to the smaller effective sample

size. Results for additional estimands, which were qualitatively similar, and measures of the networks’ similarity can be found in Appendix F.

We conducted additional bias-variance simulations in semi-experimental settings by taking the four social networks from Paluck et al. (2016) study (see Section 7 for more details on the networks) as \mathcal{A} , and simulating treatments and outcomes with the same DGP as in our first set of simulations in this study while taking the main network used by Paluck et al. (2016) as the true network. The results are qualitatively the same as those reported here (Appendix F).

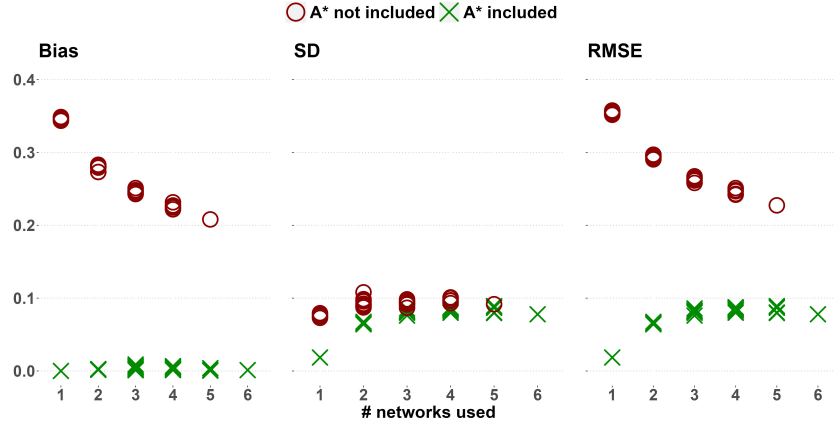


Figure 3: Bias-variance tradeoff of the NMR Hajek estimator for $\tau(c_{11}, c_{10})$ as captured by absolute bias, SD, and RMSE. X ’s indicate that the true network \mathcal{A}^* is included in \mathcal{A} , and O ’s otherwise. True causal effect is $\tau(c_{11}, c_{10}) = 0.5$.

7 Data analyses

7.1 Social network field experiment

We analyzed a field experiment that tested how anti-conflict norms spread in middle school social networks. Key information is provided below; full details are given in Paluck et al. (2016). Following previous analyses (Aronow and Samii, 2017), we analyzed a subset of $n = 2983$ eligible students from 56 schools. Half of the schools were randomly assigned to the intervention arm, and within each selected school, half of the eligible students were given a year-long anti-conflict educational intervention. To derive the within-school social network, students were asked to list ten students they spend time (ST) with. The questionnaires were given during the pre- and post-intervention periods. As previously discussed (Example 4), a social network of middle school students is dynamic and probably changed in the span of a year. Moreover, students’ questionnaire answers might not be an accurate representation of the interference structure (Example 1). Specifically, students were also asked to list their two best friends (BF). A network structure based on this list is different from the network structure derived from the ST list. Thus, the researchers can choose between four different

network specifications: either the ST or BF networks from either the measurement in the pre- or post-intervention periods. A network measured in the post-intervention period is a post-treatment variable, thus using it in the estimation of causal effects implies the assumption that the intervention did not affect the network structure (See Example 4).

We proceed to estimate the effect of the intervention on a behavior outcome (an indicator of wearing a wristband endorsing the program). Following Aronow and Samii (2017), we use the exposure mapping defined below, which is in the nature of (9), but also indicates whether the school was assigned to the intervention arm. Let s_i be an indicator of whether the school of unit i was included in the intervention arm. Let $g(\mathbf{z}, \mathbf{A}_i)$ denote the proportion of treated neighbors of unit i (as defined before (9)). The exposure mapping is

$$f(\mathbf{z}, \mathbf{A}_i) = \begin{cases} c_{111}, & z_i \mathbb{I}\{g(\mathbf{z}, \mathbf{A}_i) > 0\} s_i = 1 \\ c_{011}, & (1 - z_i) \mathbb{I}\{g(\mathbf{z}, \mathbf{A}_i) > 0\} s_i = 1 \\ c_{101}, & z_i (1 - \mathbb{I}\{g(\mathbf{z}, \mathbf{A}_i) > 0\}) s_i = 1 \\ c_{001}, & (1 - z_i) (1 - \mathbb{I}\{g(\mathbf{z}, \mathbf{A}_i) > 0\}) s_i = 1 \\ c_{000}, & (1 - s_i) = 1 \end{cases}$$

In our analysis, we estimated the causal effects with each of the four networks separately, with both pre-intervention networks, and with all four networks simultaneously with the NMR estimators.

Table 1 displays the estimated school participation effect $\tau(c_{001}, c_{000})$ and the direct isolated effect $\tau(c_{101}, c_{000})$ coupled with conservative standard errors (SEs) estimates. The BF network resulted in a larger estimated SE than the ST network due to the sparser network structure. The Hajek point estimates were larger and had smaller SEs than HT estimators across all setups. A surprising result is that for the Hajek estimator, the point estimates were similar using the four networks separately and simultaneously, but those estimates varied more in HT, perhaps due to the instability of the weights. Looking at the Hajek estimates, we can conclude that both $\tau(c_{001}, c_{000})$ and $\tau(c_{101}, c_{000})$ were found to have a small positive value, and the results were robust to the four possible specifications of the network structure. Results from different network combinations and additional estimands are given in Appendix F.

Table 1: Estimated causal effects in the social network field experiment. Results are reported as point estimates (SE). “ALL” is the four networks combined and is estimated with the NMR estimators.

| Networks | $\tau(c_{001}, c_{000})$ | | $\tau(c_{101}, c_{000})$ | |
|-----------------|--------------------------|---------------|--------------------------|---------------|
| | HT | Hajek | HT | Hajek |
| ST-pre | 0.061 (0.217) | 0.146 (0.164) | 0.096 (0.272) | 0.271 (0.190) |
| BF-pre | 0.084 (0.254) | 0.123 (0.195) | 0.169 (0.361) | 0.265 (0.254) |
| ST-post | 0.060 (0.214) | 0.131 (0.164) | 0.116 (0.298) | 0.252 (0.212) |
| BF-post | 0.090 (0.262) | 0.135 (0.200) | 0.170 (0.362) | 0.258 (0.256) |
| ST-pre & BF-pre | 0.051 (0.198) | 0.134 (0.151) | 0.079 (0.247) | 0.261 (0.175) |
| ALL | 0.040 (0.177) | 0.178 (0.131) | 0.046 (0.190) | 0.227 (0.137) |

7.2 Cluster-randomized trial

We analyzed a CRT that tested how educational intervention affects depression and anxiety symptoms among secondary school students in Kenya (Venturo-Conerly et al., 2022). The study included 895 students from two schools with 12 classes each. Classes were randomly assigned to one of four different treatment arms: *Growth*, *Value*, *Gratitude*, and *Control*. The outcome is the difference in the Generalized Anxiety Disorder Screener (GAD). The experiment consisted of a single-session educational intervention followed by a re-measurement of GAD two weeks later. Venturo-Conerly et al. (2022) found a significant effect only with the *Growth* and *Value* interventions, thus we defined binary treatment z_i that equal to one only if student i was assigned to *Growth* or *Value* interventions.

We addressed the concern that students from different classes, at the same school, can interact and share insights from the intervention, thus leading to contamination between clusters (classes). Therefore, we applied the PBA proposed in Section 5.2 to examine how cross-clusters contamination may have changed the results. The baseline network \mathbf{A}^C has the structure of 24 well-separated clusters, where all units are fully connected within each cluster. We assessed the impact of contamination with PBA under three different network deviation distributions $q(\mathbf{A}^*|\mathbf{A}^C, \boldsymbol{\theta})$. Contamination is postulated to be possible only within the school. Specifically, we assumed that $\Pr(A_{ij}^* = 1 | A_{ij}^C = 0) = \mathbb{I}\{\text{school}_i = \text{school}_j\}\theta_{ij}$ independently among units, and considered three scenarios for the cross-clusters edge creation probability θ_{ij} .

- (I) Same probability for all pairs of units: $\theta_{ij} = \theta, \forall i, j$.
- (II) Unique probability for each pair: different θ_{ij} for all i, j .
- (III) Probability that depends on the unit's gender: $\theta_{ij} = \theta_0 + \mathbb{I}\{\text{gender}_i = \text{gender}_j\}\theta_1$.

In Scenarios (I) and (II), each pair of students from a different class, at the same school, was connected with either the same or different probability, respectively. In Scenario (III), the probability was postulated to depend on a baseline value θ_0 and on θ_1 that determines whether students of the same gender are more or less likely to form social connections that can result in treatment interference.

Initially, the distribution of the bias parameters was assumed to be Uniform. Namely, in Scenarios (I) and (II), both θ and θ_{ij} were assumed to follow a $U[0, 0.005]$ distribution. In Scenario (III), we took $\theta_0 \sim U[0, 0.003]$ and $\theta_1 \sim U[0, 0.002]$ implying that students of the same gender are more likely to interact. To test the sensitivity to the bias parameter distribution choice, we repeated Scenarios (I) and (II) with more informative $Beta(0.25, 25)$ distribution which is more concentrated around zero but larger values of θ_i and θ_{ij} were possible compared to the postulated Uniform distributions. We assumed the exposure mapping (9) with $\nu_i = 0$ and focused on estimating the overall treatment effect $\tau(c_{11}, c_{00})$ (see Appendix D for more details on estimands in CRTs).

Figure 4 displays the results of the PBA with 10^3 iterations. Results are shown with and without incorporation of random error. The “Baseline” results show the Hajek point estimate and 95% confidence interval computed assuming no contamination, i.e., when the specified network is \mathbf{A}^C . The confidence interval is computed with the conservative variance estimator and based on asymptotic normal distribution (Aronow and Samii, 2017). The “Baseline” confidence interval accounts only for random error (i.e., uncertainty from treatment allocation). Turning to the PBA, the results are presented as the mean and [2.5%, 97.5%] percentiles of the Hajek estimates. The mean of point estimates in all scenarios and bias parameter distribution choices are found to be similar to the no-contamination baseline. Accounting only for the systematic error of contamination yields shorter intervals. Adding random error as described in Section 5.2, increases dramatically the uncertainty across the mean estimate. Accounting for both systematic and random error yields wider intervals than under the no-contamination baseline. Replacing the Uniform distribution with Beta distribution in Scenario (I) and (II) yields wider intervals, with minimal change to the mean estimates. Nonetheless, the random error uncertainty quantification may be overestimated due to the conservative nature of the variance estimator used (Appendix C & F). Results from PBA of Scenario (I) with $q(\boldsymbol{\theta})$ being a point-mass distribution $q(\boldsymbol{\theta}) = \mathbb{I}\{\boldsymbol{\theta} = \boldsymbol{\theta}^\dagger\}$ for $\boldsymbol{\theta}^\dagger \in \{0.0005, 0.001, \dots, 0.005\}$ are given in Appendix F.

In conclusion, although the mean PBA estimates were similar to the point estimate assuming no contamination, if moderate levels of contamination are suspected (as expressed in the choice of our bias distributions), conclusions regarding the causal effects are less informative. These results are consistent across all the bias distributions we considered.

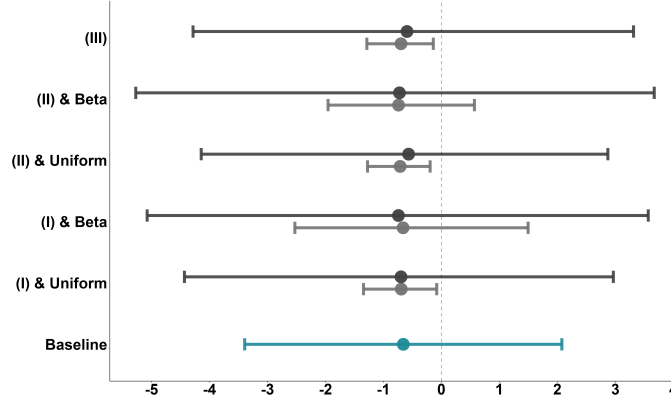


Figure 4: Probabilistic bias analysis for cross-clusters contamination under various bias parameter distributions. “Baseline” show the Hajek point estimate [95% CI] assuming no contamination. For the rest, the results from the PBA with 10^3 iterations are presented as the mean and [2.5%, 97.5%] percentiles of the Hajek estimates. Results are shown without (light gray) and with (dark gray) incorporation of random error via normal approximation and conservative variance estimator.

8 Discussion

In this paper, we studied the estimation of causal effects with a misspecified network interference structure. Building on the exposure mapping framework, we found that the correctly specified network is not necessarily unique, and that uniqueness is guaranteed under strong conditions. Motivated by our results on the bias arising from using a wrong network, we proposed two practical solutions. We first proposed the NMR estimator that allows estimation using multiple networks simultaneously and showed that it is unbiased if at least one of the networks is correctly specified. The bias-variance tradeoff of the NMR estimators was demonstrated in a simulation study. As a second practical tool, we also presented a PBA framework when researchers have a single network and can postulate a suspected misspecification mechanism. Such an approach is attractive when researchers have in mind potential deviations from the assumed network and would like to assess how they impact the causal estimates. One prominent scenario is a CRT with possible cross-clusters contamination, for which we provided a data analysis example illustrating our proposed approach.

For simplicity, we assumed that the interference network is undirected and unweighted. That assumption is often implausible. Researchers can relax it by modifying the exposure mapping, e.g., to depend differently on in- and out-edges. All the theoretical results and proposed remedies for network misspecification are expected to hold for directed and weighted networks as well. Furthermore, the neighborhood interference assumption (1) is often implausible, as interference between higher-order neighbors can be present. One option is to define a modified network $\mathbf{A}' := (\mathbf{A}^{sp})^k$ for some natural number k that represents the order of postulated interference. Another option is to allow the interference to decay with the geodesic distance of the network (Leung, 2022).

Taking the exposure mapping to be a map between treatments and networks to exposure levels enabled us to discern between two types of exposure mapping misspecification: incorrect map and wrong network. The former was previously studied (Aronow and Samii, 2017; Sävje, 2023). In practice, it is plausible that both the map and the network are incorrect. Randomization tests under interference have been developed to test exposure mapping specification without distinguishing whether the mapping or network is misspecified (Bowers et al., 2013; Athey et al., 2018; Basse et al., 2019; Puelz et al., 2022; Hoshino and Yanagi, 2023). Athey et al. (2018) also considered the null hypothesis that only one network among two “competing networks” is correctly specified. One potential approach involves adapting these randomization tests for testing the joint null hypothesis of correctly specified network and correct mapping. This can be achieved by testing the intersection of multiple null hypotheses of exposure mapping specifications, e.g., by modifying the “exclusion restriction” condition proposed by Puelz et al. (2022). However, computational and power limitations may arise when implementing such tests, highlighting an important area for future research.

When researchers worry that both the network and the map are misspecified, the NMR estimator can still be used to estimate the *expected exposure effect* as defined by Sävje (2023), which does not assume the exposure mapping is correct. Furthermore, if, for a given network, researchers can postulate different exposure mapping with the same image space \mathcal{C} , but are unsure which map is correct, a modified NMR estimator that estimates causal effects only on units with the same exposure value under all mapping can be constructed. Under additional assumptions on the class of exposure mappings, such an estimator will be unbiased if one of the mappings is correct, thus providing robustness to exposure mapping specification in general.

The NMR estimator was shown to be unbiased when at least one network is correctly specified, but its variance increases with the number of networks. Mitigating the bias-variance tradeoff can be accomplished by, e.g., using an interpolation between the NMR estimator and the naive, single-network estimators. Denote the M available networks by $\mathcal{A} = \{\mathbf{A}^1, \dots, \mathbf{A}^M\}$. The NMR is $\hat{\mu}_{\mathcal{A}}$ and each of the naive estimators are $\hat{\mu}_{\mathbf{A}^m}$, $m = 1, \dots, M$. Interpolation can be accomplished, for example, by taking weight $\omega \in [0, 1]$ of the NMR and $1 - \omega$ of the mean of naive estimators:

$$\hat{\mu}_{int}(c_\ell) = \omega \hat{\mu}_{\mathcal{A}}(c_\ell) + (1 - \omega) \frac{1}{M} \sum_{m=1}^M \hat{\mu}_{\mathbf{A}^m}(c_\ell).$$

Nevertheless, if not all networks in \mathcal{A} are correctly specified, $\hat{\mu}_{int}(c_k)$ will be biased (by the additivity of expectation), but perhaps will have a smaller variance than the NMR estimator. Finding ω that solves the bias-variance tradeoff (e.g., by minimizing the RMSE) will be ideal. However, such ω will depend on both the expectation and the variance of $\hat{\mu}_{\mathbf{A}^m}$ which can not be computed or unbiasedly estimated whenever some \mathbf{A}^m are not correctly specified (Appendix A & C).

The proposed PBA framework flexibly incorporates uncertainty in the specified network into the causal estimates. PBA, by construction, is only approximate Bayesian. Note that the network deviation distribution can be expressed as $q(\mathbf{A}^* | \mathbf{A}^{sp}) \propto q(\mathbf{A}^{sp} | \mathbf{A}^*) q(\mathbf{A}^*)$, where the dependence on $\boldsymbol{\theta}$ is omitted for brevity. Therefore, a full Bayesian analysis that accounts for uncertainty in the specified network requires a network model $q(\mathbf{A}^*)$ and a misspecification mechanism $q(\mathbf{A}^{sp} | \mathbf{A}^*)$. Coupled with an outcome model, a Bayesian analysis enables estimating causal effects while accounting for possible uncertainty in the specified network. Extending the design-based framework to a model-based Bayesian analysis is thus a natural extension of our paper.

In the simulation study, we considered the heterogeneous thresholds exposure mapping (9). Estimation of the thresholds, and the exposure mapping in general, is an interesting area for future research and has only been done in linear parametric settings (Tran and Zheleva, 2022). Misspecification of the interference network might result from a partial set of nodes (units) or an incorrect set of edges (for a given set of nodes). Using a subsample

of units in a network yields a bias even when treatment is randomized (Chandrasekhar and Lewis, 2011). In this paper, we focused only on the impact of an incorrect set of edges. Causal inference with misspecification of the network’s structure due to missing nodes is another area for future research.

Interference is the norm rather than the exception in many social domains, such as economics, political science, sociology, and infectious disease epidemiology. However, causal inference with interference raises various technical and conceptual difficulties. To address these challenges, rigorous applications must acknowledge and address the limitations that arise from interference. Our work is a step towards achieving this goal.

References

- Aronow, P. M. and Middleton, J. A. (2013). A class of unbiased estimators of the average treatment effect in randomized experiments. *Journal of Causal Inference*, 1(1):135–154.
- Aronow, P. M. and Samii, C. (2013). Conservative variance estimation for sampling designs with zero pairwise inclusion probabilities. *Survey Methodology*, 39(1):231–241.
- Aronow, P. M. and Samii, C. (2017). Estimating average causal effects under general interference, with application to a social network experiment. *The Annals of Applied Statistics*, 11(4).
- Athey, S., Eckles, D., and Imbens, G. W. (2018). Exact p-values for network interference. *Journal of the American Statistical Association*, 113(521):230–240.
- Barabási, A.-L. and Albert, R. (1999). Emergence of scaling in random networks. *Science*, 286(5439):509–512.
- Basse, G. W. and Airolidi, E. M. (2018). Limitations of design-based causal inference and a/b testing under arbitrary and network interference. *Sociological Methodology*, 48(1):136–151.
- Basse, G. W., Feller, A., and Toulis, P. (2019). Randomization tests of causal effects under interference. *Biometrika*, 106(2):487–494.
- Bhattacharya, R., Malinsky, D., and Shpitser, I. (2020). Causal inference under interference and network uncertainty. In *Uncertainty in Artificial Intelligence*, pages 1028–1038. PMLR.
- Borm, G. F., Melis, R. J. F., Teerenstra, S., and Peer, P. G. (2005). Pseudo cluster randomization: a treatment allocation method to minimize contamination and selection bias. *Statistics in Medicine*, 24(23):3535–3547.
- Boucher, V. and Houndetoungan, E. A. (2022). Estimating peer effects using partial network data. *Centre de recherche sur les risques les enjeux économiques et les politiques*.
- Bowers, J., Fredrickson, M. M., and Panagopoulos, C. (2013). Reasoning about interference between units: A general framework. *Political Analysis*, 21(1):97–124.
- Cai, J., Janvry, A. D., and Sadoulet, E. (2015). Social networks and the decision to insure. *American Economic Journal: Applied Economics*, 7(2):81–108.
- Chandrasekhar, A. and Lewis, R. (2011). Econometrics of sampled networks. *Unpublished manuscript, MIT*. [422].
- Cortez, M., Eichhorn, M., and Yu, C. (2022). Staggered rollout designs enable causal inference under interference without network knowledge. In *Advances in Neural Information Processing Systems*.

- Cox, D. R. (1958). *Planning of experiments*. Wiley, New York.
- Ebel, H., Davidsen, J., and Bornholdt, S. (2002). Dynamics of social networks. *Complexity*, 8(2):24–27.
- Egami, N. (2020). Spillover effects in the presence of unobserved networks. *Political Analysis*, 29(3):287–316.
- Forastiere, L., Airolidi, E. M., and Mealli, F. (2020). Identification and estimation of treatment and interference effects in observational studies on networks. *Journal of the American Statistical Association*, 116(534):901–918.
- Fox, M. P., MacLehose, R. F., and Lash, T. L. (2021). *Applying Quantitative Bias Analysis to Epidemiologic Data*. Statistics for Biology and Health. Springer, Cham, 2nd ed. 2021. edition.
- Greenland, S. (2005). Multiple-Bias Modelling for Analysis of Observational Data. *Journal of the Royal Statistical Society Series A: Statistics in Society*, 168(2):267–306.
- Griffith, A. (2021). Name your friends, but only five? the importance of censoring in peer effects estimates using social network data. *Journal of Labor Economics*.
- Halloran, M. E. and Struchiner, C. J. (1991). Study designs for dependent happenings. *Epidemiology*, 2(5):331–338.
- Halloran, M. E. and Struchiner, C. J. (1995). Causal inference in infectious diseases. *Epidemiology*, 6(2):142–151.
- Hardy, M., Heath, R. M., Lee, W., and McCormick, T. H. (2019). Estimating spillovers using imprecisely measured networks. *arXiv preprint arXiv:1904.00136*.
- Hartley, H. O. and Ross, A. (1954). Unbiased ratio estimators. *Nature*, 174(4423):270–271.
- Hayek, S., Shaham, G., Ben-Shlomo, Y., Kepten, E., Dagan, N., Nevo, D., Lipsitch, M., Reis, B. Y., Balicer, R. D., and Barda, N. (2022). Indirect protection of children from sars-cov-2 infection through parental vaccination. *Science*, 375(6585):1155–1159.
- Holland, P. W., Laskey, K. B., and Leinhardt, S. (1983). Stochastic blockmodels: First steps. *Social Networks*, 5(2):109–137.
- Hong, G. and Raudenbush, S. W. (2006). Evaluating kindergarten retention policy. *Journal of the American Statistical Association*, 101(475):901–910.
- Hoshino, T. and Yanagi, T. (2023). Randomization test for the specification of interference structure. *arXiv preprint arXiv:2301.05580*.
- Hu, Y., Li, S., and Wager, S. (2022). Average direct and indirect causal effects under interference. *Biometrika*.
- Hudgens, M. G. and Halloran, M. E. (2008). Toward causal inference with interference. *Journal of the American Statistical Association*, 103(482):832–842.
- Lash, T. L. and Fink, A. K. (2003). Semi-Automated Sensitivity Analysis to Assess Systematic Errors in Observational Data. *Epidemiology*, 14(4):451.
- Leung, M. P. (2020). Treatment and spillover effects under network interference. *The Review of Economics and Statistics*, 102(2):368–380.
- Leung, M. P. (2022). Causal inference under approximate neighborhood interference. *Econometrica*, 90(1):267–293, <https://onlinelibrary.wiley.com/doi/pdf/10.3982/ECTA17841>.

- Li, W., Sussman, D. L., and Kolaczyk, E. D. (2021). Causal inference under network interference with noise. *arXiv preprint arXiv:2105.04518*.
- MacLehose, R. F. and Gustafson, P. (2012). Is Probabilistic Bias Analysis Approximately Bayesian? *Epidemiology*, 23(1):151.
- Manski, C. F. (1993). Identification of endogenous social effects: The reflection problem. *The Review of Economic Studies*, 60(3):531.
- Manski, C. F. (2013). Identification of treatment response with social interactions. *The Econometrics Journal*, 16(1):S1–S23.
- Nagarajan, K., Muniyandi, M., Palani, B., and Sellappan, S. (2020). Social network analysis methods for exploring SARS-CoV-2 contact tracing data. *BMC Medical Research Methodology*, 20(1).
- Neyman, J. (1923). Sur les applications de la thar des probabilités aux expériences agricoles: essai des principes. [*English translation of excerpts (1990) by D. Dabrowska and T. Speed, Statistical Science*, 5, 463–472.].
- Ogburn, E. L., Sofrygin, O., Díaz, I., and van der Laan, M. J. (2022). Causal inference for social network data. *Journal of the American Statistical Association*, pages 1–46, <https://doi.org/10.1080/01621459.2022.2131557>.
- Paluck, E. L., Shepherd, H., and Aronow, P. M. (2016). Changing climates of conflict: A social network experiment in 56 schools. *Proceedings of the National Academy of Sciences*, 113(3):566–571, <https://www.pnas.org/doi/pdf/10.1073/pnas.1514483113>.
- Puelz, D., Basse, G., Feller, A., and Toulis, P. (2022). A graph-theoretic approach to randomization tests of causal effects under general interference. *Journal of the Royal Statistical Society: Series B (Statistical Methodology)*, 84(1):174–204.
- Rosenbaum, P. R. (2002). *Observational studies*. Springer series in statistics. Springer, New York, 2. ed. edition.
- Rosenbaum, P. R. (2007). Interference between units in randomized experiments. *Journal of the American Statistical Association*, 102(477):191–200.
- Schaefer, D. R., Haas, S. A., and Bishop, N. J. (2012). A dynamic model of US adolescents’ smoking and friendship networks. *American Journal of Public Health*, 102(6):e12–e18.
- Särndal, C.-E., Swensson, B., and Wretman, J. (2003). *Model Assisted Survey Sampling (Springer Series in Statistics)*. Springer.
- Sävje, F. (2023). Causal inference with misspecified exposure mappings: separating definitions and assumptions. *Biometrika*.
- Sävje, F., Aronow, P. M., and Hudgens, M. G. (2021). Average treatment effects in the presence of unknown interference. *The Annals of Statistics*, 49(2).
- Tchetgen Tchetgen, E. J., Fulcher, I. R., and Shpitser, I. (2020). Auto-g-computation of causal effects on a network. *Journal of the American Statistical Association*, 116(534):833–844.
- Tchetgen Tchetgen, E. J. and VanderWeele, T. J. (2012). On causal inference in the presence of interference. *Statistical Methods in Medical Research*, 21(1):55–75.
- Tortú, C., Crimaldi, I., Mealli, F., and Forastiere, L. (2021). Causal effects with hidden treatment diffusion on observed or partially observed networks. *arXiv preprint arXiv:2109.07502*.
- Tran, C. and Zheleva, E. (2022). Heterogeneous peer effects in the linear threshold model. *arXiv preprint arXiv:2201.11242*.

- Ugander, J., Karrer, B., Backstrom, L., and Kleinberg, J. (2013). Graph cluster randomization: Network exposure to multiple universes. In *Proceedings of the 19th ACM SIGKDD international conference on Knowledge discovery and data mining*, pages 329–337.
- Venturo-Conerly, K. E., Osborn, T. L., Alemu, R., Roe, E., Rodriguez, M., Gan, J., Arango, S., Wasil, A., Wasanga, C., and Weisz, J. R. (2022). Single-session interventions for adolescent anxiety and depression symptoms in kenya: A cluster-randomized controlled trial. *Behaviour Research and Therapy*, 151:104040.
- Yu, C. L., Airoidi, E. M., Borgs, C., and Chayes, J. T. (2022). Estimating the total treatment effect in randomized experiments with unknown network structure. *Proceedings of the National Academy of Sciences*, 119(44).

Appendix

A Proofs

A.1 Proof of Proposition 1

Proof. Assume in contradiction there exists another network $\mathbf{A} \in \mathcal{A}$ that satisfies Definition 2, which is not \mathbf{A}^* (i.e., $\mathbf{A}^* \neq \mathbf{A}$). Assumption 1 implies there exists $\mathbf{z} \in \mathcal{Z}$ such that $f(\mathbf{z}, \mathbf{A}_i^*) = c_\ell$ and $f(\mathbf{z}, \mathbf{A}_i) = c_k$, for some i and some $\ell \neq k$. By Definition 2, we have that $Y_i(\mathbf{z}) = \tilde{Y}_i(c_\ell)$ and $Y_i(\mathbf{z}) = \tilde{Y}_i(c_k)$, i.e., $\tilde{Y}_i(c_\ell) = \tilde{Y}_i(c_k)$. However this is in contradiction to Assumption 2, thus it must be that $\mathbf{A}^* = \mathbf{A}$. \square

A.2 The heterogeneous thresholds exposure mapping satisfies Assumption 1

Proposition A.1. *Assumption 1 holds for the exposure mapping (9).*

Proof. Let $\mathbf{A} \neq \mathbf{A}' \in \mathcal{A}$. Since $\mathbf{A} \neq \mathbf{A}'$, there exists some unit i with $\mathbf{A}_i \neq \mathbf{A}'_i$. The difference between \mathbf{A}_i and \mathbf{A}'_i can be due to the addition or removal of at least one edge. Let $d_i(\mathbf{A}) = |\mathcal{N}_i(\mathbf{A})|$ be the degree of unit i in network \mathbf{A} . Assume that $d_i(\mathbf{A}) = a$ and $d_i(\mathbf{A}') = a'$, for some scalars $a, a' \in \mathbb{N}$. Assume WLOG that $a \geq a'$.

Denote the set of joint edges of i in the two networks by $\mathcal{M}_i(\mathbf{A}, \mathbf{A}') = \mathcal{N}_i(\mathbf{A}) \cap \mathcal{N}_i(\mathbf{A}')$. Denote the complementary set of $\mathcal{N}_i(\mathbf{A})$, excluding i itself, by $\mathcal{N}_i(\mathbf{A})^c = \{j \neq i : A_{ij} = 0\}$, and similarly for $\mathcal{N}_i(\mathbf{A}')^c$. Denote the edges difference set by $\mathcal{N}_i(\mathbf{A}) \setminus \mathcal{N}_i(\mathbf{A}') = \mathcal{N}_i(\mathbf{A}) \cap \mathcal{N}_i(\mathbf{A}')^c$. We may write $\mathcal{N}_i(\mathbf{A})$ as

$$\begin{aligned} \mathcal{N}_i(\mathbf{A}) &= [\mathcal{N}_i(\mathbf{A}) \cap \mathcal{N}_i(\mathbf{A}')^c] \cup [\mathcal{N}_i(\mathbf{A}) \cap \mathcal{N}_i(\mathbf{A}')] \\ &= [\mathcal{N}_i(\mathbf{A}) \cap \mathcal{N}_i(\mathbf{A}')^c] \cup \mathcal{M}_i(\mathbf{A}, \mathbf{A}') \end{aligned}$$

Since $\mathcal{N}_i(\mathbf{A}) \cap \mathcal{N}_i(\mathbf{A}')^c$ and $\mathcal{M}_i(\mathbf{A}, \mathbf{A}')$ are disjoint, we can write $g(\mathbf{z}, \mathbf{A}_i)$ as

$$g(\mathbf{z}, \mathbf{A}_i) = \frac{1}{a} \left(\sum_{j \in \mathcal{N}_i(\mathbf{A}) \cap \mathcal{N}_i(\mathbf{A}')^c} z_j + \sum_{j \in \mathcal{M}_i(\mathbf{A}, \mathbf{A}')} z_j \right),$$

and similarly for $g(\mathbf{z}, \mathbf{A}'_i)$,

$$g(\mathbf{z}, \mathbf{A}'_i) = \frac{1}{a'} \left(\sum_{j \in \mathcal{N}_i(\mathbf{A}') \cap \mathcal{N}_i(\mathbf{A})^c} z_j + \sum_{j \in \mathcal{M}_i(\mathbf{A}, \mathbf{A}')} z_j \right).$$

Since $a \geq a'$, the set $\mathcal{N}_i(\mathbf{A}) \cap \mathcal{N}_i(\mathbf{A}')^c$ is not empty. Now, taking \mathbf{z} with $z_i = 1$, the possible exposure values are only c_{10} and c_{11} . We separate the proof for the two possible cases and further separate as needed. We show that in each of these (sub) cases, one can choose a treatments vector \mathbf{z} such that $f(\mathbf{z}, \mathbf{A}_i) \neq f(\mathbf{z}, \mathbf{A}'_i)$ (e.g., under one network we obtain exposure level c_{11} and under the other one c_{10}). Turning to the different cases, we start with separating the cases $\nu_i = 0$ and $\nu_i > 0$

1. Case 1: $\nu_i = 0$. Here we can take $z_j = 0$ for all $j \in [\mathcal{N}_i(\mathbf{A}') \cap \mathcal{N}_i(\mathbf{A})^c] \cup \mathcal{M}_i(\mathbf{A}, \mathbf{A}')$, and $z_j = 1$ for at least one $j \in \mathcal{N}_i(\mathbf{A}) \cap \mathcal{N}_i(\mathbf{A}')^c$, to obtain a specific treatment vector \mathbf{z} that results with $g(\mathbf{z}, \mathbf{A}_i) > 0$ and $g(\mathbf{z}, \mathbf{A}'_i) = 0$, and therefore $f(\mathbf{z}, \mathbf{A}_i) = c_{11}$, while $f(\mathbf{z}, \mathbf{A}'_i) = c_{10}$, as required.
2. Case 2: $0 < \nu_i < 1$. Denote the number of edges in each of the aforementioned sets by $n_{i,a} = |\mathcal{N}_i(\mathbf{A}) \cap \mathcal{N}_i(\mathbf{A}')^c|$, $n_{i,a'} = |\mathcal{N}_i(\mathbf{A}') \cap \mathcal{N}_i(\mathbf{A})^c|$, $n_{i,a \cap a'} = |\mathcal{M}_i(\mathbf{A}, \mathbf{A}')|$. We obtain that $n_{i,a} + n_{i,a \cap a'} = a$, $n_{i,a'} + n_{i,a \cap a'} = a'$, and $n_{i,a} \geq 1$. We differentiate between two cases.
 - i. If $\frac{n_{i,a}}{a} > \nu_i$ then for $z_j = 1$ for all $j \in \mathcal{N}_i(\mathbf{A}) \cap \mathcal{N}_i(\mathbf{A}')^c$, and $z_j = 0$ for the rest, we obtain $g(\mathbf{z}, \mathbf{A}_i) > \nu_i$ while $g(\mathbf{z}, \mathbf{A}'_i) = 0 < \nu_i$, as required.
 - ii. If $\frac{n_{i,a}}{a} \leq \nu_i$, from positivity of all exposure values under both \mathbf{A} and \mathbf{A}' , there must exist a set of units in $\mathcal{N}_i(\mathbf{A})$ such that $g(\mathbf{z}, \mathbf{A}_i) > 0$. Since $\frac{n_{i,a}}{a} \leq \nu_i$, we have to add treated units from $\mathcal{M}_i(\mathbf{A}, \mathbf{A}')$ for $g(\mathbf{z}, \mathbf{A}_i)$ to be larger than ν_i , thus $\mathcal{M}_i(\mathbf{A}, \mathbf{A}')$ is not an empty set. Define the minimal number of such units by

$$\tilde{n}_{i,a \cap a'} = \min_{\tilde{n} \in \{1, \dots, n_{i,a \cap a'}\}} \tilde{n}, \text{ s.t. } \frac{n_{i,a} + \tilde{n}}{a} > \nu_i \quad (\text{A.1})$$

Here we also have two options.

- If $\frac{\tilde{n}_{i,a \cap a'}}{a'} \leq \nu_i$, we can take, $z_j = 1$ for all $j \in \mathcal{N}_i(\mathbf{A}) \cap \mathcal{N}_i(\mathbf{A}')^c$ and for $\tilde{n}_{i,a \cap a'}$ units from $\mathcal{M}_i(\mathbf{A}, \mathbf{A}')$ to obtain $g(\mathbf{z}, \mathbf{A}_i) > \nu_i$ and $g(\mathbf{z}, \mathbf{A}'_i) \leq \nu_i$, as required.
- If $\frac{\tilde{n}_{i,a \cap a'}}{a'} > \nu_i$, now the previous treatments selection yields $g(\mathbf{z}, \mathbf{A}'_i) > \nu_i$. However, notice that $\tilde{n}_{i,a \cap a'}$ as defined in (A.1), is *minimal*, i.e., $\frac{n_{i,a} + \tilde{n}_{i,a \cap a'}}{a} > \nu_i$ and $\frac{n_{i,a} + \tilde{n}_{i,a \cap a'} - 1}{a} \leq \nu_i$. Therefore,

$$\frac{\tilde{n}_{i,a \cap a'}}{a} \leq \nu_i - \frac{n_{i,a} - 1}{a} \leq \nu_i, \quad (\text{A.2})$$

where the last inequality in (A.2) holds since $n_{i,a} \geq 1$. Thus, if we take $z_j = 1$ for $\tilde{n}_{i,a \cap a'}$ units from $\mathcal{M}_i(\mathbf{A}, \mathbf{A}')$, and $z_j = 0$ for the rest, we obtain $g(\mathbf{z}, \mathbf{A}_i) \leq \nu_i$ and $g(\mathbf{z}, \mathbf{A}'_i) > \nu_i$, as required.

□

A.3 Proof of Theorem 1

Proof. Let \mathbf{A}^{sp} be the specified network. Let $\mathbf{A}^* \in \mathcal{A}^*$ be some correctly specified network. By consistency,

$$\begin{aligned}
\mathbb{E}_{\mathbf{Z}} [\hat{\mu}_{\mathbf{A}^{sp}}(c_k)] &= \mathbb{E}_{\mathbf{Z}} \left[\frac{1}{n} \sum_{i=1}^n \mathbb{I}\{f(\mathbf{Z}, \mathbf{A}_i^{sp}) = c_k\} \frac{1}{p_i^{(\mathbf{A}^{sp})}(c_k)} \sum_{j=1}^L \mathbb{I}\{f(\mathbf{Z}, \mathbf{A}_i^*) = c_j\} \tilde{Y}_i(c_j) \right] \\
&= \frac{1}{n} \mathbb{E}_{\mathbf{Z}} \left[\sum_{i=1}^n \sum_{j=1}^L \frac{1}{p_i^{(\mathbf{A}^{sp})}(c_k)} \mathbb{I}\{f(\mathbf{Z}, \mathbf{A}_i^{sp}) = c_k\} \mathbb{I}\{f(\mathbf{Z}, \mathbf{A}_i^*) = c_j\} \tilde{Y}_i(c_j) \right] \\
&= \frac{1}{n} \sum_{i=1}^n \sum_{j=1}^L \frac{1}{p_i^{(\mathbf{A}^{sp})}(c_k)} \mathbb{E}_{\mathbf{Z}} \left[\mathbb{I}\{f(\mathbf{Z}, \mathbf{A}_i^{sp}) = c_k\} \mathbb{I}\{f(\mathbf{Z}, \mathbf{A}_i^*) = c_j\} \right] \tilde{Y}_i(c_j) \\
&= \frac{1}{n} \sum_{i=1}^n \sum_{j=1}^L \frac{p_i^{(\mathbf{A}^*, \mathbf{A}^{sp})}(c_j, c_k)}{p_i^{(\mathbf{A}^{sp})}(c_k)} \tilde{Y}_i(c_j). \\
&= \frac{1}{n} \sum_{i=1}^n \sum_{j=1}^L p_i(c_j; \mathbf{A}^* \mid c_k; \mathbf{A}^{sp}) \tilde{Y}_i(c_j)
\end{aligned}$$

By adding and subtracting $\mu(c_k)$ we obtain,

$$\mathbb{E}_{\mathbf{Z}} [\hat{\mu}_{\mathbf{A}^{sp}}(c_k)] = \mu(c_k) + \frac{1}{n} \sum_{i=1}^n \left[\{p_i(c_k; \mathbf{A}^* \mid c_k; \mathbf{A}^{sp}) - 1\} \tilde{Y}_i(c_k) + \sum_{j=1, j \neq k}^L p_i(c_j; \mathbf{A}^* \mid c_k; \mathbf{A}^{sp}) \tilde{Y}_i(c_j) \right]$$

Rearranging and taking absolute values on both sides yields,

$$\begin{aligned}
\left| \mathbb{E}_{\mathbf{Z}} [\hat{\mu}_{\mathbf{A}^{sp}}(c_k)] - \mu(c_k) \right| &= \left| \frac{1}{n} \sum_{i=1}^n \left[\{p_i(c_k; \mathbf{A}^* \mid c_k; \mathbf{A}^{sp}) - 1\} \tilde{Y}_i(c_k) + \sum_{j=1, j \neq k}^L p_i(c_j; \mathbf{A}^* \mid c_k; \mathbf{A}^{sp}) \tilde{Y}_i(c_j) \right] \right| \\
&\leq \frac{1}{n} \sum_{i=1}^n \left[|p_i(c_k; \mathbf{A}^* \mid c_k; \mathbf{A}^{sp}) - 1| \cdot |\tilde{Y}_i(c_k)| + \sum_{j=1, j \neq k}^L p_i(c_j; \mathbf{A}^* \mid c_k; \mathbf{A}^{sp}) \cdot |\tilde{Y}_i(c_j)| \right] \\
&\leq \frac{\kappa}{n} \sum_{i=1}^n \left[|p_i(c_k; \mathbf{A}^* \mid c_k; \mathbf{A}^{sp}) - 1| + \sum_{j=1, j \neq k}^L p_i(c_j; \mathbf{A}^* \mid c_k; \mathbf{A}^{sp}) \right] \\
&= \frac{\kappa}{n} \sum_{i=1}^n \left[|p_i(c_k; \mathbf{A}^* \mid c_k; \mathbf{A}^{sp}) - 1| + 1 - p_i(c_k; \mathbf{A}^* \mid c_k; \mathbf{A}^{sp}) \right] \\
&= \frac{2\kappa}{n} \sum_{i=1}^n 1 - p_i(c_k; \mathbf{A}^* \mid c_k; \mathbf{A}^{sp}),
\end{aligned}$$

where the second line follows from Minkowski's inequality, the third line from Assumption 4 of bounded potential outcomes $|Y_i(c_j)| \leq \kappa$, $\forall i, j$, the fourth line since there L possible exposures and their probabilities sum to one, and the fifth line since $|p_i(c_k; \mathbf{A}^* \mid c_k; \mathbf{A}^{sp}) - 1| = 1 - p_i(c_k; \mathbf{A}^* \mid c_k; \mathbf{A}^{sp})$. \square

Moreover, recall that the HT estimator of causal effects is $\hat{\tau}_{\mathbf{A}^{sp}}(c_\ell, c_k) = \hat{\mu}_{\mathbf{A}^{sp}}(c_\ell) - \hat{\mu}_{\mathbf{A}^{sp}}(c_k)$, and that causal effects are defined as $\tau(c_\ell, c_k) = \mu(c_\ell) - \mu(c_k)$. Therefore,

$$\begin{aligned} \left| \mathbb{E}_{\mathbf{Z}} [\hat{\tau}_{\mathbf{A}^{sp}}(c_\ell, c_k)] - \tau(c_\ell, c_k) \right| &= \left| \mathbb{E}_{\mathbf{Z}} [\hat{\mu}_{\mathbf{A}^{sp}}(c_\ell) - \hat{\mu}_{\mathbf{A}^{sp}}(c_k)] - \{\mu(c_\ell) - \mu(c_k)\} \right| \\ &= \left| \left\{ \mathbb{E}_{\mathbf{Z}} [\hat{\mu}_{\mathbf{A}^{sp}}(c_\ell)] - \mu(c_\ell) \right\} + \left\{ \mu(c_k) - \mathbb{E}_{\mathbf{Z}} [\hat{\mu}_{\mathbf{A}^{sp}}(c_k)] \right\} \right| \\ &\leq \left| \mathbb{E}_{\mathbf{Z}} [\hat{\mu}_{\mathbf{A}^{sp}}(c_\ell)] - \mu(c_\ell) \right| + \left| \mu(c_k) - \mathbb{E}_{\mathbf{Z}} [\hat{\mu}_{\mathbf{A}^{sp}}(c_k)] \right| \\ &= \left| \mathbb{E}_{\mathbf{Z}} [\hat{\mu}_{\mathbf{A}^{sp}}(c_\ell)] - \mu(c_\ell) \right| + \left| \mathbb{E}_{\mathbf{Z}} [\hat{\mu}_{\mathbf{A}^{sp}}(c_k)] - \mu(c_k) \right| \end{aligned}$$

Consequently, by Theorem 1,

$$\left| \mathbb{E}_{\mathbf{Z}} [\hat{\tau}_{\mathbf{A}^{sp}}(c_\ell, c_k)] - \tau(c_\ell, c_k) \right| \leq \frac{2\kappa}{n} \sum_{i=1}^n \{1 - p_i(c_\ell; \mathbf{A}^* \mid c_\ell; \mathbf{A}^{sp})\} + \{1 - p_i(c_k; \mathbf{A}^* \mid c_k; \mathbf{A}^{sp})\}$$

A.4 Exact bias of the Horvitz-Thompson estimator

In this subsection we derive the exact bias of $\hat{\tau}_{\mathbf{A}^{sp}}(c_\ell, c_k)$. To that end, we can relax Assumption 4 of bounded potential outcomes. From the proof of Theorem 1 shown in the previous subsection

$$\mathbb{E}_{\mathbf{Z}} [\hat{\mu}_{\mathbf{A}^{sp}}(c_k)] = \frac{1}{n} \sum_{i=1}^n \sum_{j=1}^L p_i(c_j; \mathbf{A}^* \mid c_k; \mathbf{A}^{sp}) \tilde{Y}_i(c_j),$$

therefore,

$$\begin{aligned} \mathbb{E}_{\mathbf{Z}} [\hat{\tau}_{\mathbf{A}^{sp}}(c_\ell, c_k)] &= \mathbb{E}_{\mathbf{Z}} [\hat{\mu}_{\mathbf{A}^{sp}}(c_\ell) - \hat{\mu}_{\mathbf{A}^{sp}}(c_k)] \\ &= \frac{1}{n} \sum_{i=1}^n \sum_{j=1}^L [p_i(c_j; \mathbf{A}^* \mid c_\ell; \mathbf{A}^{sp}) - p_i(c_j; \mathbf{A}^* \mid c_k; \mathbf{A}^{sp})] \tilde{Y}_i(c_j) \\ &= \frac{1}{n} \sum_{i=1}^n \sum_{j=1}^L [p_i(c_j; \mathbf{A}^* \mid c_\ell; \mathbf{A}^{sp}) - p_i(c_j; \mathbf{A}^* \mid c_k; \mathbf{A}^{sp})] \tilde{Y}_i(c_j) \\ &\quad + \tau(c_\ell, c_k) - \tau(c_\ell, c_k) \\ &= \tau(c_\ell, c_k) + \frac{1}{n} \sum_{i=1}^n \sum_{j=1}^L [q_i(c_j; \mathbf{A}^* \mid c_\ell; \mathbf{A}^{sp}) - q_i(c_j; \mathbf{A}^* \mid c_k; \mathbf{A}^{sp})] \tilde{Y}_i(c_j) \\ &= \tau(c_\ell, c_k) + B(c_\ell, c_k; \mathbf{A}^{sp}), \end{aligned}$$

with

$$B(c_\ell, c_k; \mathbf{A}^{sp}) = \frac{1}{n} \sum_{i=1}^n \sum_{j=1}^L [q_i(c_j; \mathbf{A}^* \mid c_\ell; \mathbf{A}^{sp}) - q_i(c_j; \mathbf{A}^* \mid c_k; \mathbf{A}^{sp})] \tilde{Y}_i(c_j),$$

and where q_i are defined by

$$q_i(c_j; \mathbf{A}^* | c_k; \mathbf{A}^{sp}) = \begin{cases} p_i(c_j; \mathbf{A}^* | c_k; \mathbf{A}^{sp}), & j \neq k \\ p_i(c_j; \mathbf{A}^* | c_k; \mathbf{A}^{sp}) - 1, & j = k \end{cases}$$

That is, that bias of $\hat{\tau}_{\mathbf{A}^{sp}}$ is a weighted sum of all L potential outcomes \tilde{Y} with weights that relates to the conditional probabilities $p_i(c_j; \mathbf{A}^* | c_k; \mathbf{A}^{sp})$.

Moreover, as shown in Section 3, the sum $\sum_{j=1}^L \mathbb{I}\{f(\mathbf{Z}, \mathbf{A}_i^*) = c_j\} \tilde{Y}_i(c_j)$ is equal for all $\mathbf{A}^* \in \mathcal{A}^*$. Thus, the term $\mathbb{I}\{f(\mathbf{Z}, \mathbf{A}_i^{sp}) = c_k\} \sum_{j=1}^L \mathbb{I}\{f(\mathbf{Z}, \mathbf{A}_i^*) = c_j\} \tilde{Y}_i(c_j)$ is also equal for all $\mathbf{A}^* \in \mathcal{A}^*$, and by taking expectation w.r.t. \mathbf{Z} we obtain that $B(c_\ell, c_k; \mathbf{A}^{sp})$ is equal for all $\mathbf{A}^* \in \mathcal{A}^*$.

A.5 Proof of Theorem 2

Proof. Let $\mathcal{A} = \{\mathbf{A}^1, \dots, \mathbf{A}^M\}$ be the collection of M networks. Note that $\mathcal{A} \cap \mathcal{A}^* \neq \emptyset$ means that for some j , $\mathbf{A}^j \in \mathcal{A}^*$. Assume without loss of generality that $\mathbf{A}^1 \in \mathcal{A}^*$ and

write $\mathbf{A}^1 = \mathbf{A}^*$. We obtain

$$\begin{aligned}
\mathbb{E}_{\mathbf{Z}} [\hat{\mu}_{\mathcal{A}}(c_\ell)] &= \mathbb{E}_{\mathbf{Z}} \left[\frac{1}{n} \sum_{i=1}^n \left(\prod_{j=1}^M \mathbb{I}\{f(\mathbf{Z}, \mathbf{A}_i^j) = c_\ell\} \right) \frac{1}{p_i^{(\mathcal{A})}(c_\ell)} Y_i^o \right] \\
(\text{Consistency}) &= \mathbb{E}_{\mathbf{Z}} \left[\frac{1}{n} \sum_{i=1}^n \left(\prod_{j=1}^M \mathbb{I}\{f(\mathbf{Z}, \mathbf{A}_i^j) = c_\ell\} \right) \frac{1}{p_i^{(\mathcal{A})}(c_\ell)} \sum_{k=1}^L \mathbb{I}\{f(\mathbf{Z}, \mathbf{A}_i^*) = c_k\} \tilde{Y}_i(c_k) \right] \\
&= \mathbb{E}_{\mathbf{Z}} \left[\frac{1}{n} \sum_{i=1}^n \left(\prod_{j=2}^M \mathbb{I}\{f(\mathbf{Z}, \mathbf{A}_i^j) = c_\ell\} \right) \frac{1}{p_i^{(\mathcal{A})}(c_\ell)} \cdot \right. \\
&\quad \left. \mathbb{I}\{f(\mathbf{Z}, \mathbf{A}_i^1) = c_\ell\} \sum_{k=1}^L \mathbb{I}\{f(\mathbf{Z}, \mathbf{A}_i^*) = c_k\} \tilde{Y}_i(c_k) \right] \\
(\mathbf{A}^1 = \mathbf{A}^*) &= \mathbb{E}_{\mathbf{Z}} \left[\frac{1}{n} \sum_{i=1}^n \left(\prod_{j=2}^M \mathbb{I}\{f(\mathbf{Z}, \mathbf{A}_i^j) = c_\ell\} \right) \frac{1}{p_i^{(\mathcal{A})}(c_\ell)} \cdot \right. \\
&\quad \left. \sum_{k=1}^L \mathbb{I}\{f(\mathbf{Z}, \mathbf{A}_i^*) = c_\ell\} \mathbb{I}\{f(\mathbf{Z}, \mathbf{A}_i^*) = c_k\} \tilde{Y}_i(c_k) \right] \\
&\stackrel{\dagger}{=} \mathbb{E}_{\mathbf{Z}} \left[\frac{1}{n} \sum_{i=1}^n \left(\prod_{j=1}^M \mathbb{I}\{f(\mathbf{Z}, \mathbf{A}_i^j) = c_\ell\} \right) \frac{1}{p_i^{(\mathcal{A})}(c_\ell)} \tilde{Y}_i(c_\ell) \right] \\
&= \frac{1}{n} \sum_{i=1}^n \mathbb{E}_{\mathbf{Z}} \left[\prod_{j=1}^M \mathbb{I}\{f(\mathbf{Z}, \mathbf{A}_i^j) = c_\ell\} \right] \frac{1}{p_i^{(\mathcal{A})}(c_\ell)} \tilde{Y}_i(c_\ell) \\
&= \frac{1}{n} \sum_{i=1}^n p_i^{(\mathcal{A})}(c_\ell) \frac{1}{p_i^{(\mathcal{A})}(c_\ell)} \tilde{Y}_i(c_\ell) \\
&= \frac{1}{n} \sum_{i=1}^n \tilde{Y}_i(c_\ell) \\
&= \mu(c_\ell)
\end{aligned}$$

Where \dagger follows from the fact that $\sum_{k=1}^L \mathbb{I}\{f(\mathbf{Z}, \mathbf{A}_i^*) = c_\ell\} \mathbb{I}\{f(\mathbf{Z}, \mathbf{A}_i^*) = c_k\} \tilde{Y}_i(c_k) = \mathbb{I}\{f(\mathbf{Z}, \mathbf{A}_i^*) = c_\ell\} \tilde{Y}_i(c_\ell)$. Moreover, if \mathbf{A}^* is not unique (i.e., \mathcal{A}^* is not a singleton), the sum $\sum_{k=1}^L \mathbb{I}\{f(\mathbf{Z}, \mathbf{A}_i^*) = c_k\} \tilde{Y}_i(c_k)$ will be equal for any $\mathbf{A}^* \in \mathcal{A}^*$, as already been established in the main text (Section 3), and thus the proof will follow using similar derivations. The additivity of expectation yields

$$\mathbb{E}_{\mathbf{Z}} [\hat{\tau}_{\mathcal{A}}(c_\ell, c_k)] = \mathbb{E}_{\mathbf{Z}} [\hat{\mu}_{\mathcal{A}}(c_\ell)] - \mathbb{E}_{\mathbf{Z}} [\hat{\mu}_{\mathcal{A}}(c_k)] = \mu(c_\ell) - \mu(c_k) = \tau(c_\ell, c_k).$$

□

B Bounds on Hajek estimator bias

We consider here the NMR Hajek estimator ((8) in the main text) since it is a generalization of the common Hajek estimator (4). As in the proof of Theorem 2, let $\mathcal{A} = \{\mathbf{A}^1, \dots, \mathbf{A}^M\}$ be the collection of M networks. Assume that $\mathbf{A}^j \in \mathcal{A}^*$ for some j . The Hajek estimator is given by

$$\hat{\mu}_{\mathcal{A}}^H(c_\ell) = \frac{\sum_{i=1}^n I_i^{(\mathcal{A})}(\mathbf{Z}^o, c_\ell) \frac{1}{p_i^{(\mathcal{A})}(c_\ell)} Y_i^o}{\sum_{i=1}^n I_i^{(\mathcal{A})}(\mathbf{Z}^o, c_\ell) \frac{1}{p_i^{(\mathcal{A})}(c_\ell)}} = \frac{V_1}{V_2}$$

with V_1 being the numerator and V_2 the denominator. As already been established in Appendix A,

$$\begin{aligned} \mathbb{E}_{\mathbf{Z}}[V_1] &= \mathbb{E}_{\mathbf{Z}} \left[\sum_{i=1}^n I_i^{(\mathcal{A})}(\mathbf{Z}^o, c_\ell) \frac{1}{p_i^{(\mathcal{A})}(c_\ell)} Y_i^o \right] = \sum_{i=1}^n \tilde{Y}_i(c_\ell) \\ \mathbb{E}_{\mathbf{Z}}[V_2] &= \mathbb{E}_{\mathbf{Z}} \left[\sum_{i=1}^n I_i^{(\mathcal{A})}(\mathbf{Z}^o, c_\ell) \frac{1}{p_i^{(\mathcal{A})}(c_\ell)} \right] = n \end{aligned}$$

Thus, $\frac{\mathbb{E}_{\mathbf{Z}}[V_1]}{\mathbb{E}_{\mathbf{Z}}[V_2]} = \mu(c_\ell)$, i.e., the Hajek estimator is the ratio of two unbiased estimators. However, such a ratio is not unbiased in itself. The bias bound of the Hajek ratio estimator is proportional to the variance of V_1 and V_2 (Hartley and Ross, 1954; Särndal et al., 2003)

$$\left| \hat{\mu}_{\mathcal{A}}^H(c_\ell) - \mu(c_\ell) \right| \leq \sqrt{\text{Var}_{\mathbf{Z}}(V_1) \text{Var}_{\mathbf{Z}}(V_2)}. \quad (\text{B.1})$$

Under some limitation on the asymptotic network structure, it can be shown that the bias bound (B.1) converges to zero (Ugander et al., 2013; Aronow and Samii, 2017; Sävje, 2023; Li et al., 2021).

C Variance of the NMR estimators

In this section, we derive the variance of the NMR estimators, and, following Aronow and Samii (2013), suggest a conservative variance estimator.

As in the proof of Theorem 2, let $\mathcal{A} = \{\mathbf{A}^1, \dots, \mathbf{A}^M\}$ be the collection of M networks. We also denote for brevity $Y_i = Y_i^o$. Assume throughout that $\mathbf{A}^j \in \mathcal{A}^*$ for some j , i.e., \mathcal{A} contains a correctly specified network. Define $p_{ij}^{(\mathcal{A})}(c_\ell, c_k) = \mathbb{E}_{\mathbf{Z}} \left[I_i^{(\mathcal{A})}(\mathbf{Z}, c_\ell) I_j^{(\mathcal{A})}(\mathbf{Z}, c_k) \right]$ as the joint probability that units i, j have exposure values c_ℓ, c_k , respectively, under all the networks in \mathcal{A} , and for brevity denote $p_{ij}^{(\mathcal{A})}(c_\ell, c_\ell) = p_{ij}^{(\mathcal{A})}(c_\ell)$. The variance of the HT NMR estimator $\hat{\tau}_{\mathcal{A}}$ (7) is given by (Särndal et al., 2003)

$$\text{Var}_{\mathbf{Z}} \left[\hat{\tau}_{\mathcal{A}}(c_k, c_\ell) \right] = \text{Var}_{\mathbf{Z}} \left[\hat{\mu}_{\mathcal{A}}(c_k) \right] + \text{Var}_{\mathbf{Z}} \left[\hat{\mu}_{\mathcal{A}}(c_\ell) \right] - 2 \text{Cov}_{\mathbf{Z}} \left[\hat{\mu}_{\mathcal{A}}(c_k), \hat{\mu}_{\mathcal{A}}(c_\ell) \right], \quad (\text{C.1})$$

with

$$\begin{aligned}
Var_{\mathbf{Z}} \left[\hat{\mu}_{\mathcal{A}}(c_\ell) \right] &= n^{-2} \sum_{i=1}^n p_i^{(\mathcal{A})}(c_\ell) \left(1 - p_i^{(\mathcal{A})}(c_\ell) \right) \left(\frac{\tilde{Y}_i(c_\ell)}{p_i^{(\mathcal{A})}(c_\ell)} \right)^2 \\
&\quad + n^{-2} \sum_{i=1}^n \sum_{j \in \{j \mid j \neq i, p_{ij}^{(\mathcal{A})}(c_\ell) > 0\}} \left(p_{ij}^{(\mathcal{A})}(c_\ell) - p_i^{(\mathcal{A})}(c_\ell) p_j^{(\mathcal{A})}(c_\ell) \right) \frac{\tilde{Y}_i(c_\ell) \tilde{Y}_j(c_\ell)}{p_i^{(\mathcal{A})}(c_\ell) p_j^{(\mathcal{A})}(c_\ell)} \\
&\quad - n^{-2} \sum_{i=1}^n \sum_{j \in \{j \mid j \neq i, p_{ij}^{(\mathcal{A})}(c_\ell) = 0\}} \tilde{Y}_i(c_\ell) \tilde{Y}_j(c_\ell),
\end{aligned} \tag{C.2}$$

and,

$$\begin{aligned}
Cov_{\mathbf{Z}} \left[\hat{\mu}_{\mathcal{A}}(c_k), \hat{\mu}_{\mathcal{A}}(c_\ell) \right] &= n^{-2} \sum_{i=1}^n \sum_{j \in \{j \mid j \neq i, p_{ij}^{(\mathcal{A})}(c_k, c_\ell) > 0\}} \left(p_{ij}^{(\mathcal{A})}(c_k, c_\ell) - p_i^{(\mathcal{A})}(c_k) p_j^{(\mathcal{A})}(c_\ell) \right) \frac{\tilde{Y}_i(c_k) \tilde{Y}_j(c_\ell)}{p_i^{(\mathcal{A})}(c_k) p_j^{(\mathcal{A})}(c_\ell)} \\
&\quad - n^{-2} \sum_{i=1}^n \sum_{j \in \{j \mid p_{ij}^{(\mathcal{A})}(c_k, c_\ell) = 0\}} \tilde{Y}_i(c_k) \tilde{Y}_j(c_\ell).
\end{aligned} \tag{C.3}$$

The first two terms in the variance (C.2) and the first term in the covariance (C.3) can be estimated in an unbiased manner using an unbiased Horvitz-Thompson estimator (Aronow and Samii, 2013). However, the third term in (C.2) and the second term in (C.3) involve potential outcomes that have zero probabilities to be jointly observed ($p_{ij}^{(\mathcal{A})} = 0$), and thus, these terms are not directly estimable from the observed data. We follow Aronow and Samii (2013) and use a conservative estimator that utilizes Young's inequality. The inequality states that

$$\frac{a^r}{r} + \frac{b^q}{q} \geq ab, \quad \text{for } a, b > 0, \text{ and } \frac{1}{r} + \frac{1}{q} = 1, r, q > 0.$$

Thus, for $r = q = 2$

$$\frac{\tilde{Y}_i(c_k)^2}{2} + \frac{\tilde{Y}_j(c_\ell)^2}{2} = \frac{|\tilde{Y}_i(c_k)|^2}{2} + \frac{|\tilde{Y}_j(c_\ell)|^2}{2} \geq |\tilde{Y}_i(c_k)| \cdot |\tilde{Y}_j(c_\ell)|$$

Since any two numbers x, y satisfies $|x||y| \geq xy$ and $|x||y| \geq -xy$, we obtain the bounds

$$- \sum_{i=1}^n \sum_{j=1}^n \tilde{Y}_i(c_\ell) \tilde{Y}_j(c_\ell) \leq \sum_{i=1}^n \sum_{j=1}^n \frac{\tilde{Y}_i(c_\ell)^2}{2} + \frac{\tilde{Y}_j(c_\ell)^2}{2}, \tag{C.4}$$

$$- \sum_{i=1}^n \sum_{j=1}^n \tilde{Y}_i(c_k) \tilde{Y}_j(c_\ell) \geq - \sum_{i=1}^n \sum_{j=1}^n \frac{\tilde{Y}_i(c_k)^2}{2} + \frac{\tilde{Y}_j(c_\ell)^2}{2}, \tag{C.5}$$

and the RHS in both (C.4) and (C.5) can be estimated by an Horvitz-Thompson estimator. We can thus use the Horvitz-Thompson variance and covariance estimators

$$\begin{aligned}
\widehat{Var}[\hat{\mu}_{\mathcal{A}}(c_\ell)] &= n^{-2} \sum_{i=1}^n I_i^{(\mathcal{A})}(\mathbf{Z}, c_\ell) \left(1 - p_i^{(\mathcal{A})}(c_\ell)\right) \left(\frac{Y_i}{p_i^{(\mathcal{A})}(c_\ell)}\right)^2 \\
&\quad + n^{-2} \sum_{i=1}^n \sum_{j \in \{j \mid j \neq i, p_{ij}^{(\mathcal{A})}(c_k, c_\ell) > 0\}} \left(I_i^{(\mathcal{A})}(\mathbf{Z}, c_\ell) I_j^{(\mathcal{A})}(\mathbf{Z}, c_\ell) \cdot \frac{p_{ij}^{(\mathcal{A})}(c_\ell) - p_i^{(\mathcal{A})}(c_\ell) p_j^{(\mathcal{A})}(c_\ell)}{p_{ij}^{(\mathcal{A})}(c_\ell)} \right. \\
&\quad \left. \cdot \frac{Y_i}{p_i^{(\mathcal{A})}(c_\ell)} \cdot \frac{Y_j}{p_j^{(\mathcal{A})}(c_\ell)} \right) \\
&\quad + n^{-2} \sum_{i=1}^n \sum_{j \in \{j \mid j \neq i, p_{ij}^{(\mathcal{A})}(c_\ell) = 0\}} \left(\frac{I_i^{(\mathcal{A})}(\mathbf{Z}, c_\ell) \cdot Y_i^2}{2 \cdot p_i^{(\mathcal{A})}(c_\ell)} + \frac{I_j^{(\mathcal{A})}(\mathbf{Z}, c_\ell) \cdot Y_j^2}{2 \cdot p_j^{(\mathcal{A})}(c_\ell)} \right) \\
\widehat{Cov}[\hat{\mu}_{\mathcal{A}}(c_k), \hat{\mu}_{\mathcal{A}}(c_\ell)] &= n^{-2} \sum_i \sum_{j \in \{j \mid j \neq i, p_{ij}^{(\mathcal{A})}(c_k, c_\ell) > 0\}} \left(I_i^{(\mathcal{A})}(\mathbf{Z}, c_k) I_j^{(\mathcal{A})}(\mathbf{Z}, c_\ell) \cdot \frac{p_{ij}^{(\mathcal{A})}(c_k, c_\ell) - p_i^{(\mathcal{A})}(c_k) p_j^{(\mathcal{A})}(c_\ell)}{p_{ij}^{(\mathcal{A})}(c_k, c_\ell)} \right. \\
&\quad \left. \cdot \frac{Y_i}{p_i^{(\mathcal{A})}(c_k)} \cdot \frac{Y_j}{p_j^{(\mathcal{A})}(c_\ell)} \right) \\
&\quad - n^{-2} \sum_i \sum_{j \in \{j \mid p_{ij}^{(\mathcal{A})}(c_k, c_\ell) = 0\}} \left(\frac{I_i^{(\mathcal{A})}(\mathbf{Z}, c_k) \cdot Y_i^2}{2 \cdot p_i^{(\mathcal{A})}(c_k)} + \frac{I_j^{(\mathcal{A})}(\mathbf{Z}, c_\ell) \cdot Y_j^2}{2 \cdot p_j^{(\mathcal{A})}(c_\ell)} \right),
\end{aligned}$$

to obtain a plug-in estimator of (C.1)

$$\widehat{Var}[\hat{\tau}_{\mathcal{A}}(c_k, c_\ell)] = \widehat{Var}[\hat{\mu}_{\mathcal{A}}(c_k)] + \widehat{Var}[\hat{\mu}_{\mathcal{A}}(c_\ell)] - 2 \cdot \widehat{Cov}[\hat{\mu}_{\mathcal{A}}(c_k), \hat{\mu}_{\mathcal{A}}(c_\ell)]. \quad (\text{C.6})$$

As formally presented below, the variance estimator (C.6) is a conservative estimator.

Proposition A.2. *If $\mathbf{A}^j \in \mathcal{A}^*$ for some j , then*

$$\mathbb{E}_{\mathbf{Z}} \left[\widehat{Var}(\hat{\tau}_{\mathcal{A}}(c_k, c_\ell)) \right] \geq Var_{\mathbf{Z}} \left[\hat{\tau}_{\mathcal{A}}(c_k, c_\ell) \right], \quad k, \ell = 1, \dots, L.$$

Proof. The proof stems directly from Aronow and Samii (2013) derivations using the fact that $\mathbb{E}_{\mathbf{Z}} \left[\frac{I_i^{(\mathcal{A})}(\mathbf{Z}, c_k)}{p_i^{(\mathcal{A})}(c_k)} \right] = 1$ and that if $\mathbf{A}^j \in \mathcal{A}^*$ for some j then $I_i^{(\mathcal{A})}(\mathbf{Z}, c_k) Y_i^o = I_i^{(\mathcal{A})}(\mathbf{Z}, c_k) \tilde{Y}_i(c_k)$. \square

Variance estimation of the Hajek NMR estimator (8) is done with first order Taylor linear approximation (Särndal et al., 2003) by replacing Y_i^o in (C.6) with the residuals $U_i = Y_i^o - \hat{\mu}_{\mathcal{A}}^H(c_k)$ where c_k is the observed exposure value for unit i .

A numerical illustration of the conservativeness property via a simulation study is Appendix F.

D Estimands and estimation in cluster-randomized trials

Typically, the estimand of interest in CRTs is the overall treatment effect (OTE), which contrasts between treated and no-treated units. In CRT each treated unit is from a treated cluster, thus the OTE reduces to comparisons between treated and no-treated clusters. Extensions for two-stage randomization are possible as well (Borm et al., 2005; Hudgens and Halloran, 2008).

If we assume that each cluster forms a fully connected network, then by using the exposure mapping (9) we obtain that the OTE in CRT is equivalent to $\tau(c_{11}, c_{00})$. Note that using the exposure mapping (9) in the main text, in this case, degenerates under the contamination null since all units are exposed to either c_{11} or c_{00} by definition.

Stated formally, assume there are V clusters and denote by \mathbf{z}_v the treatment vector assigned to cluster $v = 1, \dots, V$, i.e., $\mathbf{z}_v \in \{\vec{0}, \vec{1}\}$. Then under the neighborhood interference (or exposures) assumption, $Y_i(\vec{1}) = \tilde{Y}_i(c_{11})$ and $Y_i(\vec{0}) = \tilde{Y}_i(c_{00}) \forall i$. Thus,

$$OTE = \frac{1}{n} \sum_{i=1}^n Y_i(\vec{1}) - \frac{1}{n} \sum_{i=1}^n Y_i(\vec{0}) = \frac{1}{n} \sum_{i=1}^n \tilde{Y}_i(c_{11}) - \frac{1}{n} \sum_{i=1}^n \tilde{Y}_i(c_{00}) = \tau(c_{11}, c_{00})$$

Assume that a fixed number of $0 < U < V$ clusters are selected for treatment with probabilities U/V . Let z_i be the assigned treatment at the unit level. One type of unbiased OTE estimator is of the form (Aronow and Middleton, 2013)

$$\widehat{OTE} = \frac{1}{n} \sum_{i=1}^n \frac{V}{U} z_i Y_i^o - \frac{1}{n} \sum_{i=1}^n \frac{V}{V-U} (1 - z_i) Y_i^o.$$

Let \mathbf{A} be the network representing well-separated clusters (no contamination). Under this experimental design $p_i^{(\mathbf{A})}(c_{11}) = \frac{U}{V}$ and $p_i^{(\mathbf{A})}(c_{00}) = 1 - p_i^{(\mathbf{A})}(c_{11}) = \frac{V-U}{V}$. Since z_i is binary we also obtain $\mathbb{I}\{f(Z, \mathbf{A}_i) = c_{11}\} = z_i$. We can write the HT estimator as

$$\begin{aligned} \hat{\tau}_{\mathbf{A}}(c_{11}, c_{00}) &= \frac{1}{n} \sum_{i=1}^n \mathbb{I}\{f(Z, \mathbf{A}_i) = c_{11}\} \frac{1}{p_i^{(\mathbf{A})}(c_{11})} Y_i^o - \frac{1}{n} \sum_{i=1}^n \mathbb{I}\{f(Z, \mathbf{A}_i) = c_{00}\} \frac{1}{p_i^{(\mathbf{A})}(c_{00})} Y_i^o \\ &= \frac{1}{n} \sum_{i=1}^n \frac{V}{U} z_i Y_i^o - \frac{1}{n} \sum_{i=1}^n \frac{V}{V-U} (1 - z_i) Y_i^o \\ &= \widehat{OTE} \end{aligned}$$

Thus, the HT estimator is equivalent to the common OTE estimator in CRT. We will now show that in the case of clusters with equal sizes, Hajek, HT, and OTE estimators are all equivalent. Let $I_1 \subseteq \{1, \dots, V\}$ denote the set of clusters assigned to treatment. If we

assume that all clusters are equal in size, i.e. $n_v = n/V$, $v = 1, \dots, V$, we obtain

$$\begin{aligned}
\sum_{i=1}^n \mathbb{I}\{f(Z, \mathbf{A}_i) = c_{11}\} \frac{1}{p_i^{(\mathbf{A})}(c_{11})} &= \sum_{i=1}^n \frac{V}{U} z_i \\
&= \frac{V}{U} \sum_{v \in I_1} n_v \\
&= \frac{V}{U} \sum_{v \in I_1} \frac{n}{V} \\
&= n
\end{aligned}$$

where the last equality follows since there are U clusters assigned to treatment. Similarly, $\sum_{i=1}^n \mathbb{I}\{f(Z, \mathbf{A}_i) = c_{00}\} \frac{1}{p_i^{(\mathbf{A})}(c_{00})} = n$. Thus,

$$\begin{aligned}
\hat{\tau}_{\mathbf{A}}^h(c_{11}, c_{00}) &= \frac{\sum_{i=1}^n \mathbb{I}\{f(Z, \mathbf{A}_i) = c_{11}\} \frac{1}{p_i^{(\mathbf{A})}(c_{11})} Y_i^o}{\sum_{i=1}^n \mathbb{I}\{f(Z, \mathbf{A}_i) = c_{11}\} \frac{1}{p_i^{(\mathbf{A})}(c_{11})}} \\
&\quad - \frac{\sum_{i=1}^n \mathbb{I}\{f(Z, \mathbf{A}_i) = c_{00}\} \frac{1}{p_i^{(\mathbf{A})}(c_{00})} Y_i^o}{\sum_{i=1}^n \mathbb{I}\{f(Z, \mathbf{A}_i) = c_{00}\} \frac{1}{p_i^{(\mathbf{A})}(c_{00})}} \\
&= \frac{1}{n} \sum_{i=1}^n \mathbb{I}\{f(Z, \mathbf{A}_i) = c_{11}\} \frac{1}{p_i^{(\mathbf{A})}(c_{11})} Y_i^o \\
&\quad - \frac{1}{n} \sum_{i=1}^n \mathbb{I}\{f(Z, \mathbf{A}_i) = c_{00}\} \frac{1}{p_i^{(\mathbf{A})}(c_{00})} Y_i^o \\
&= \hat{\tau}_{\mathbf{A}}(c_{11}, c_{00}) \\
&= \widehat{OTE}
\end{aligned}$$

E Cross-clusters contamination and SBM

Under the assumption of V well-separated clusters, we can represent the network as one with fully separated communities where each community is fully connected. Assume that units in different clusters $v \neq v'$ can form ties independently with probability $p_{v,v'} = p_{v',v}$. Let the edge-creating probability matrix be denoted by $Q \in \mathbb{R}^{V \times V}$ with

$$Q_{v,v'} = \begin{cases} p_{v,v'}, & v \neq v' \\ 1, & v = v' \end{cases}$$

This representation is equivalent to the stochastic block model (SBM) (Holland et al., 1983) with Q being the stochastic edge-creating matrix, and the number of communities (V) is known. Thus, assuming that contamination between clusters can be represented by Q enables one to sample a contaminated network \mathbf{A} by sampling from an SBM that is defined

by Q . Furthermore, if we let $G \in \mathbb{R}^{n \times V}$ be the unit-wise cluster indicator matrix defined by $G_{i,v} = \mathbb{I}\{\text{unit } i \text{ is in cluster } v\}$, $i = 1, \dots, n, v = 1, \dots, V$, then the expected contaminated network $\bar{\mathbf{A}} = \mathbb{E}[\mathbf{A}]$ has the form

$$\bar{\mathbf{A}} = GQG^T - \text{diag}(GQG^T)$$

F Simulations and data analyses

The R package `MisspecifiedInterference` implementing our methodology is available from https://github.com/barwein/Misspecified_Interference. Simulations and data analyses reproducibility materials of the results are available from <https://github.com/barwein/CI-MIS>.

Throughout all the simulations and data analyses performed, the exposure probabilities p_i (in each form) were estimated with $R = 10^4$ re-sampling from the relevant $\Pr(\mathbf{Z} = \mathbf{z})$. Formally, let $\mathbf{z}_1, \dots, \mathbf{z}_R$ denote the sampled treatments from $\Pr(\mathbf{Z} = \mathbf{z})$. Define the indicator matrix $I(c_\ell) \in \mathbb{R}^{n \times R}$, $\ell = 1, \dots, L$ by $I_{ij}(c_\ell) = \mathbb{I}\{f(\mathbf{z}_j, \mathbf{A}_i) = c_\ell\}$, $i = 1, \dots, n, j = 1, \dots, R$. The estimation of the exposures probabilities is performed via additive smoothing (Aronow and Samii, 2017)

$$\widehat{P}(c_\ell) = \frac{I(c_\ell)I(c_\ell)^T + I_n}{R + 1},$$

where I_n is the $n \times n$ identity matrix, and $\widehat{P}(c_\ell)$ is the estimator of $P(c_\ell)$ defined by

$$P_{ij}(c_\ell) = \begin{cases} p_i^{(\mathbf{A})}(c_\ell), & i = j \\ p_{ij}^{(\mathbf{A})}(c_\ell), & i \neq j \end{cases}$$

To express network similarity we utilized the Jaccard index. Let $\mathcal{E}(\mathbf{A})$ be the edges set of network \mathbf{A} . For two networks \mathbf{A}, \mathbf{A}' , the Jaccard index is defined by

$$J_{\mathbf{A}, \mathbf{A}'} = \frac{|\mathcal{E}(\mathbf{A}) \cap \mathcal{E}(\mathbf{A}')|}{|\mathcal{E}(\mathbf{A}) \cup \mathcal{E}(\mathbf{A}')|},$$

that is, $J_{\mathbf{A}, \mathbf{A}'}$ is the proportion of shared edges between \mathbf{A} and \mathbf{A}' to the total number of edges in \mathbf{A} or \mathbf{A}' . Thus, $0 \leq J_{\mathbf{A}, \mathbf{A}'} \leq 1$, where values close to 1 indicates that the networks are similar.

F.1 Simulations

In the simulations, a PA network of $n = 3000$ units was sampled as the baseline true network via the `igraph` package <https://igraph.org/r/> with power parameter set to 1 (Barabási and Albert, 1999). Figure F.1 displays the degree distribution of the sampled network. Clearly, the degrees distribution implies a heavy right tail, a property inherent

in the PA algorithm which is known to generate degrees that are asymptotically Pareto distributed (Barabási and Albert, 1999).

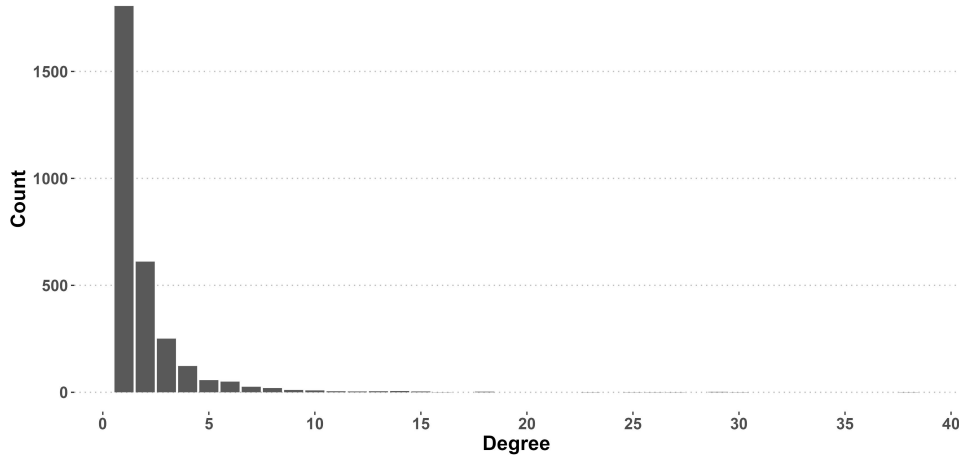


Figure F.1: Histogram of the baseline preferential attachment random network degree's distribution. $n = 3000$ nodes. The mean degree is 2, and the maximal degree is 38.

F.1.1 Illustration of the estimation bias

In this subsection, we report additional results of the simulation study shown in the main text.

Scenario (I) (Incorrect reporting of social connections). Figure F.2 shows the absolute bias for additional estimands not displayed in the main text. The results were similar. When $\eta = 0$ the bias is zero and increases with η otherwise. Moreover, Figure F.2 also shows the exact bias, as derived from Theorem 1, in comparison to the empirical bias of HT and Hajek estimators. The two are similar.

As discussed in Theorem 1, the bias from using a misspecified network structure results from selecting the wrong units and using invalid weights. Selecting the wrong units in our framework is equivalent to embedding units with the wrong exposure values. Figure F.3 shows the number of units with misclassified exposure values in the simulation. Clearly, the number of misclassified exposures increases with η , regardless of the exposure value.

The simulation validated Theorem 1 by illustrating that both Hajek and HT are unbiased whenever the network is correctly specified ($\eta = 0$). However, HT had a larger empirical standard deviation (SD) than Hajek, possibly due to the stabilizing character of estimating n when using Hajek (Särndal et al., 2003). Figure F.4 shows the empirical SD of the two estimators. We can conclude that even though both HT and Hajek had a similar bias, Hajek had a lower SD.

To quantify the similarity of \mathbf{A}^* and each of the misspecified networks, the Jaccard index was computed. Table F.1 displays the Jaccard index of \mathbf{A}^* with each sampled network (by

η). In the extreme ($\eta = 0.25$), there were only about 16% shared edges in the networks.

In the simulation, we sampled one incorrect network for each $\eta > 0$ value. To illustrate that the results are robust for replications, Figure F.5 displays the results of additional 50 replications in each we sampled different incorrect network. The bias across all replications is similar.

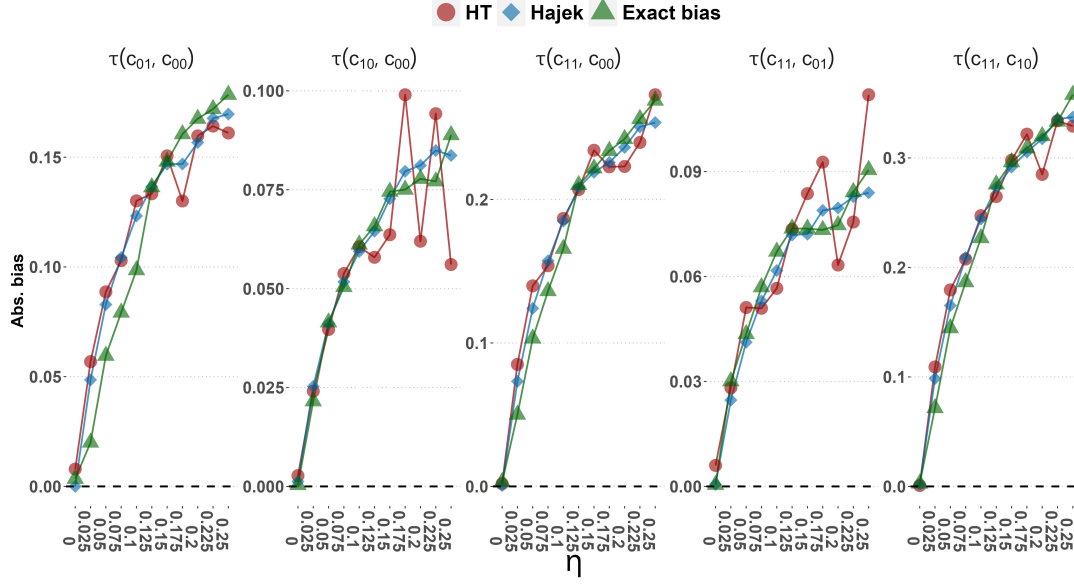


Figure F.2: Scenario (I). Additional absolute bias results from estimating $\tau(c_{01}, c_{00})$, $\tau(c_{11}, c_{00})$, $\tau(c_{11}, c_{01})$, $\tau(c_{11}, c_{10})$.

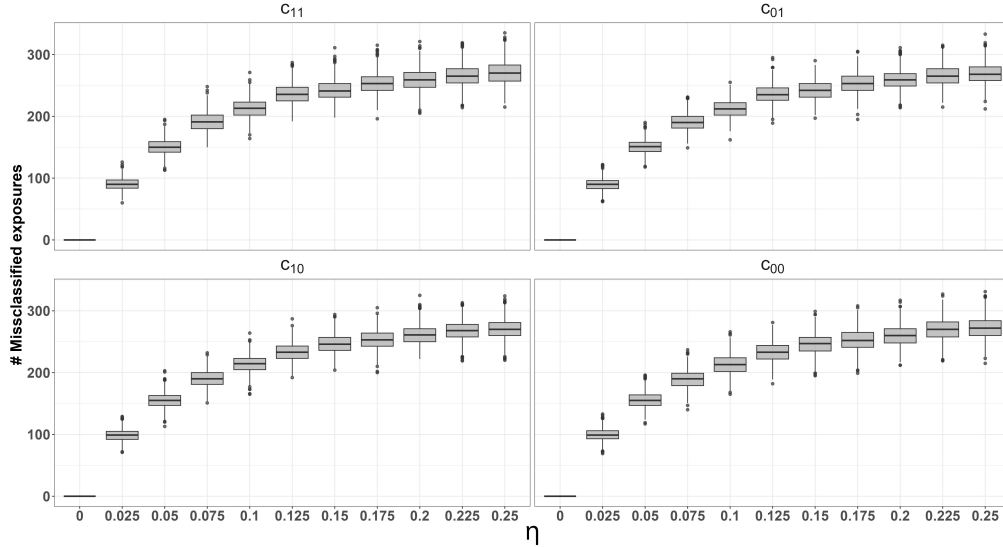


Figure F.3: Number of units with misclassified exposures by exposure value in Scenario (I).

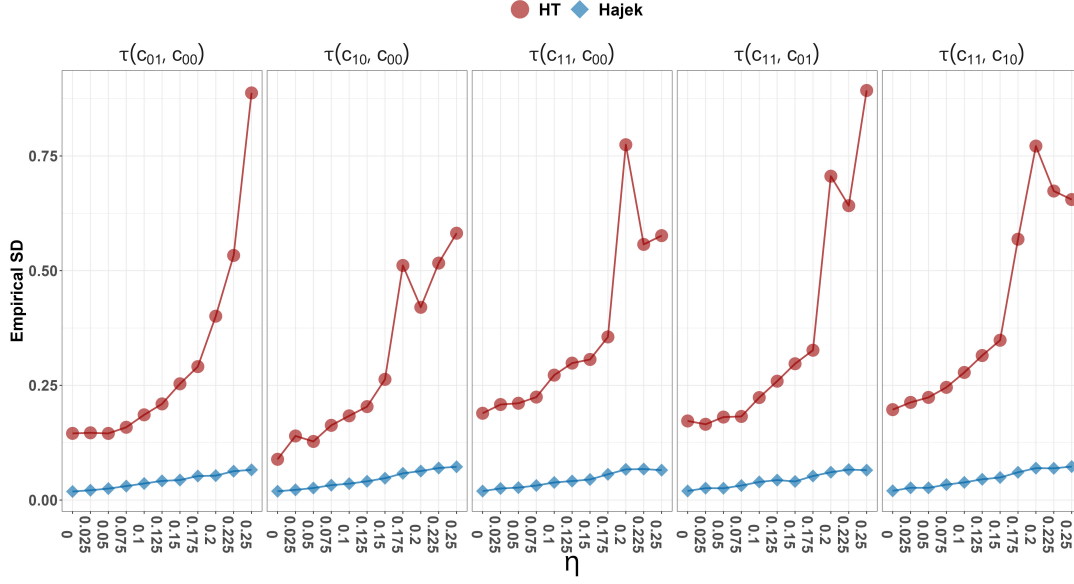


Figure F.4: Empirical standard deviation (SD) of HT and Hajek estimators in Scenario (I).

| | | | | | | | | | | | |
|--------------|---|-------|-------|-------|-------|-------|-------|-------|-------|-------|-------|
| η | 0 | 0.025 | 0.050 | 0.075 | 0.100 | 0.125 | 0.150 | 0.175 | 0.200 | 0.225 | 0.250 |
| $J_{A^*, A}$ | 1 | 0.713 | 0.545 | 0.437 | 0.365 | 0.299 | 0.261 | 0.231 | 0.203 | 0.175 | 0.163 |

Table F.1: Jaccard index of A^* and the misspecified networks in Scenario (I).

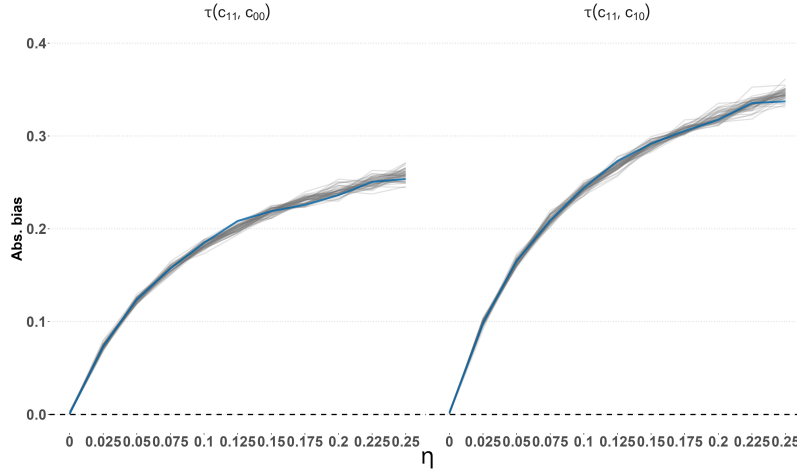


Figure F.5: Multiple replications of Scenario (I). The blue line represents the absolute bias of Hajek estimates shown in the main text, whereas each grey line results from the 50 additional replication in which different networks are sampled for each $\eta > 0$.

Scenario (II) (Censoring). Here we also report additional results similar to the ones reported in the previous scenario. Table F.2 shows the proportion of units with more than $K = 1, \dots, 7$ neighbors, i.e., the proportion of units we censored some of their edges for

each of the thresholds. For example, when $K = 7$ only about 2.5% units had censored edges, whereas when $K = 1$ almost 40% of units had censored edges. Figure F.6 shows absolute bias for additional estimands not shown in the main text. The same picture holds. When the censoring threshold K decreases, the bias increases, and the bias is larger. Notice that HT had a larger bias than Hajek when the censoring threshold K decreased, probably due to the smaller effective sample size and the weight stability of Hajek. Furthermore, the exact bias is also displayed and is similar to the empirical bias of HT and Hajek. Figure F.7 displays the number of units with misclassified exposure values by censoring threshold K . Figure F.8 shows the empirical SD of HT and Hajek estimators in Scenario (II). Here also the SD of HT is uniformly higher than Hajek. However, the SD of HT decreases with K , i.e., when more censoring is present the variance is reduced. Table F.3 provides the Jaccard index of \mathbf{A}^* and each of the censored networks. Similarly to Scenario (I), the index decreases with K . Figure F.9 shows that the results from additional 50 replications of the simulations are almost identical for those reported.

| K | 1 | 2 | 3 | 4 | 5 | 6 | 7 |
|------------------------------|-------|-------|-------|------|-------|-------|-------|
| $\Pr(d_i(\mathbf{A}^*) > K)$ | 0.398 | 0.194 | 0.111 | 0.07 | 0.051 | 0.034 | 0.025 |

Table F.2: Edges empirical right-tail function in the PA network \mathbf{A}^* . $d_i(\mathbf{A}^*)$ is the degree of unit i .

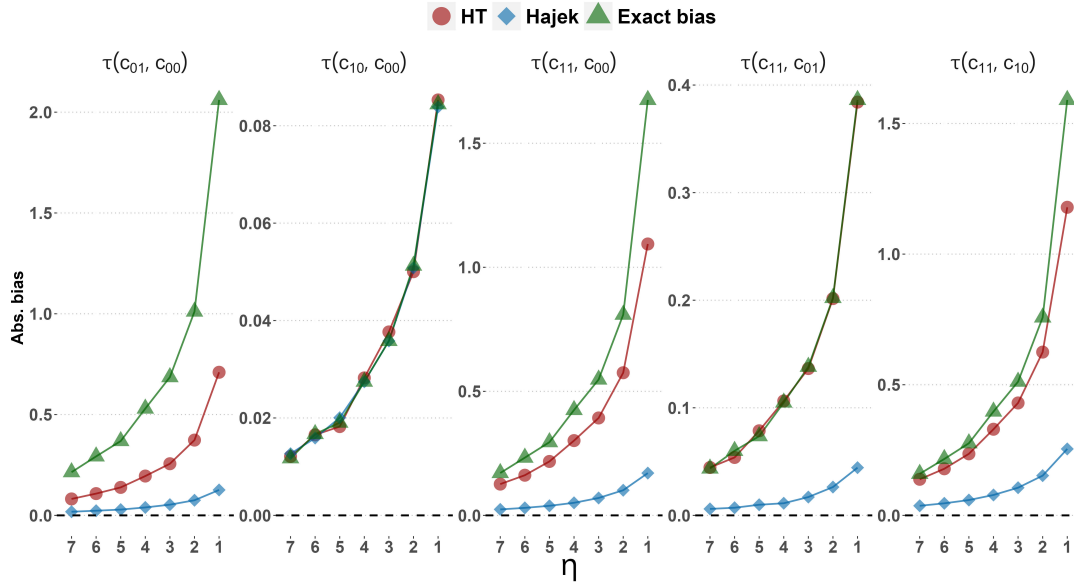


Figure F.6: Scenario (II). Additional absolute bias results from estimating $\tau(c_{01}, c_{00})$, $\tau(c_{11}, c_{00})$, $\tau(c_{11}, c_{01})$, $\tau(c_{11}, c_{10})$.

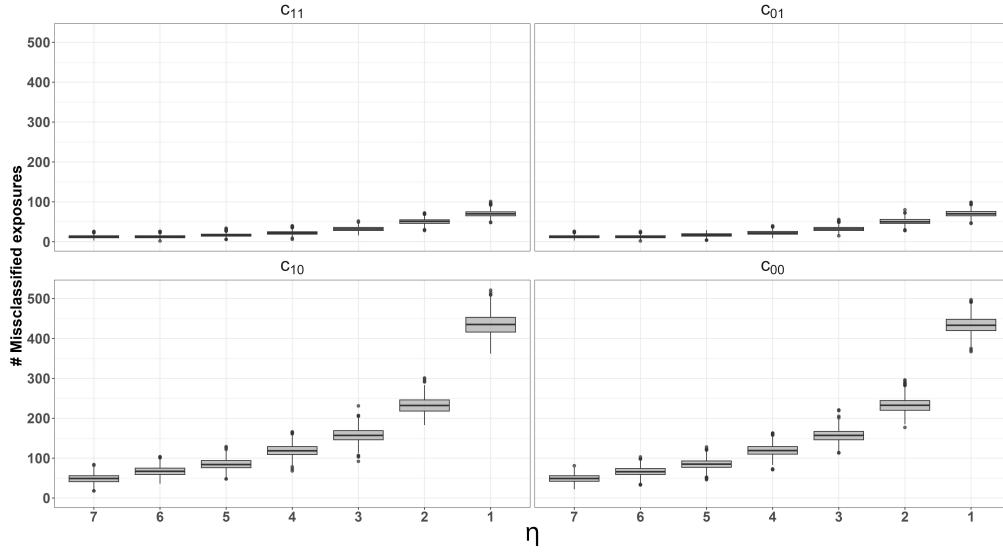


Figure F.7: Number of units with misclassified exposures by exposure value in Scenario (II).

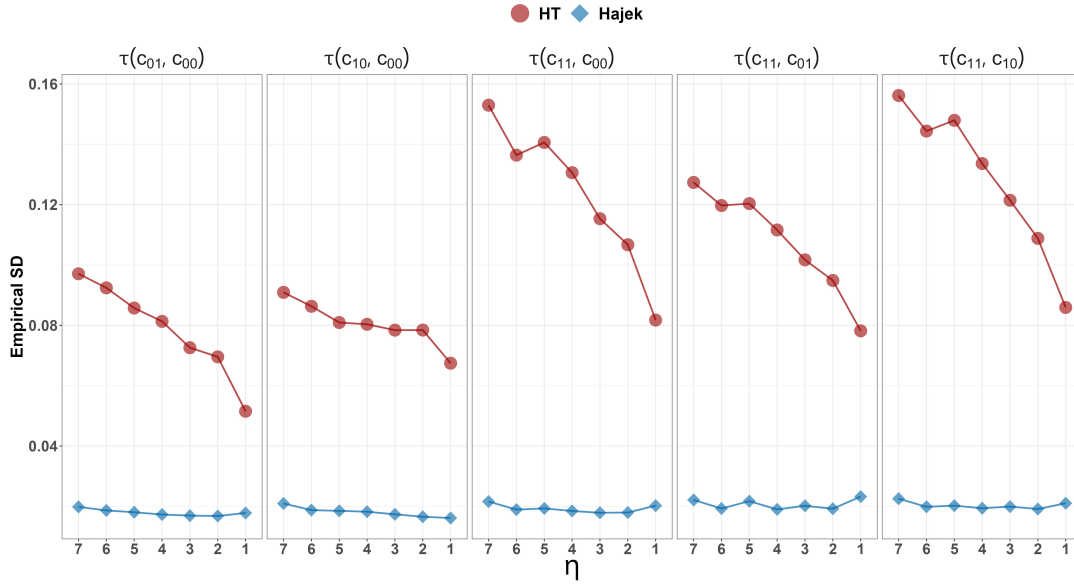


Figure F.8: Empirical standard deviation (SD) of HT and Hajek estimators in Scenario (II).

| K | 7 | 6 | 5 | 4 | 3 | 2 | 1 |
|--------------|-------|-------|-------|-------|-------|-------|-------|
| $J_{A^*, A}$ | 0.866 | 0.835 | 0.792 | 0.730 | 0.646 | 0.509 | 0.258 |

Table F.3: Jaccard index of A^* and the censored networks in Scenario (II).

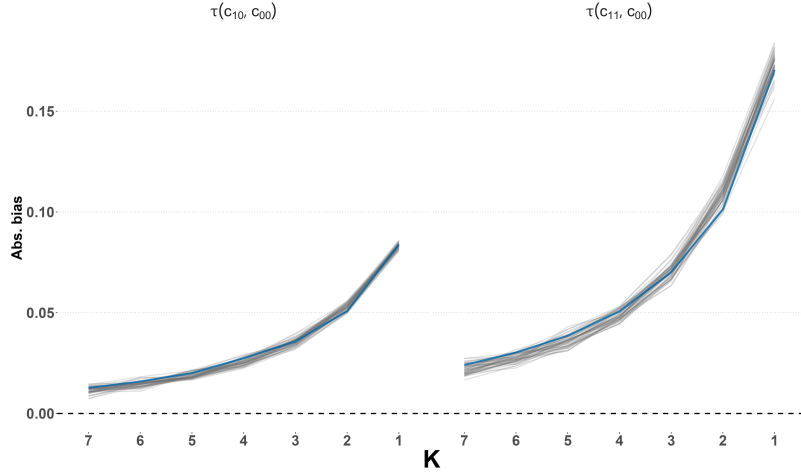


Figure F.9: Multiple replications of Scenario (II). The blue line represents the absolute bias of Hajek estimates shown in the main text, whereas each grey line results from the 50 additional replication in which different networks are sampled for each K .

Scenario (III) (Cross-clusters contamination). In the “varied” sizes scenario, cluster sizes were sampled from $U[3, 7]$ distribution.

The relation between the estimated overall treatment effect $\tau(c_{11}, c_{00})$ and common estimands in CRT is explained in Appendix D. In addition, when the contamination probabilities $p_{v,v'}$ are equal at the cluster level, i.e., not unit-specific, then the contaminated network can be modeled as a stochastic block model (SBM). Details are provided in Appendix E.

F.1.2 Bias-variance tradeoff of the NMR estimators

Figure F.10 displays additional results of the bias-variance tradeoff simulation for $\tau(c_{01}, c_{00})$ and $\tau(c_{11}, c_{00})$. Similar results to those given in the main text appear there. Table F.4 shows the pairwise Jaccard indices of all the six networks used in the simulation.

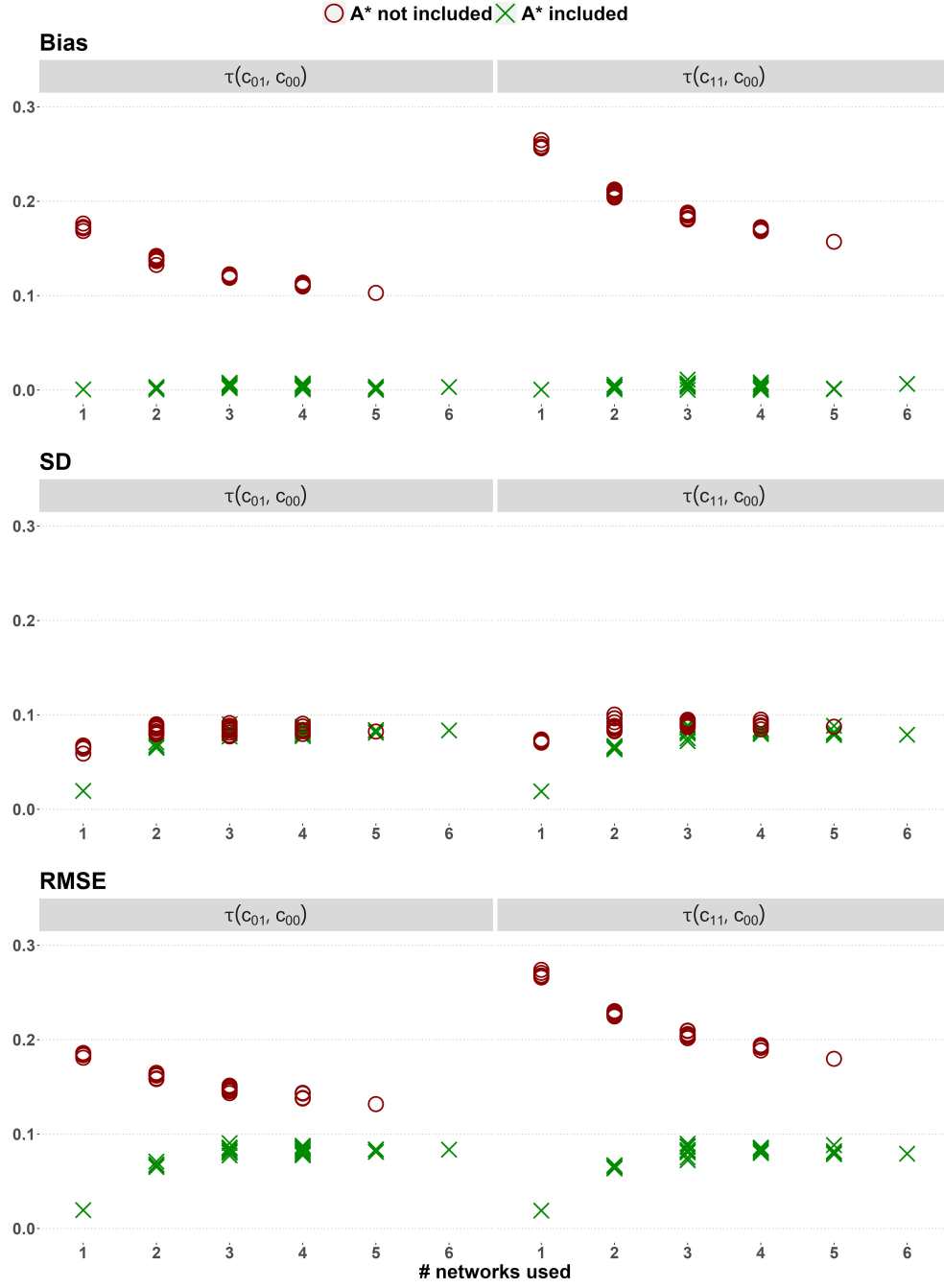


Figure F.10: Bias-variance tradeoff of the NMR estimator. The results presented are the absolute bias, SD, and RMSE estimates of the Hajek NMR estimator. True causal effects are $\tau(c_{01}, c_{00}) = 0.25$ and $\tau(c_{11}, c_{00}) = 1$.

| | A^* | A^a | A^b | A^c | A^d | A^e |
|-------|-------|-------|-------|-------|-------|-------|
| A^* | 1 | | | | | |
| A^a | 0.156 | 1 | | | | |
| A^b | 0.155 | 0.066 | 1 | | | |
| A^c | 0.159 | 0.067 | 0.066 | 1 | | |
| A^d | 0.157 | 0.067 | 0.068 | 0.068 | 1 | |
| A^e | 0.157 | 0.067 | 0.066 | 0.068 | 0.068 | 1 |

Table F.4: Jaccard index of the networks used in the simulations of the NMR bias-variance tradeoff.

Furthermore, we repeat the simulation in realistic quasi-experimental settings by taking \mathcal{A} to consists of the four available networks from Paluck et al. (2016) study, as analyzed in the data analysis section in the main text. The correct network A^* is taken to be the ST-pre network, which is the main network in Paluck et al. (2016) analysis. We used the same DGP to generate treatments and outcomes as in the previously displayed bias-variance simulations of the NMR estimators. Figure F.11 displays the results from 1000 replications. The results portray the bias-variance tradeoff inherent in the NMR estimators.

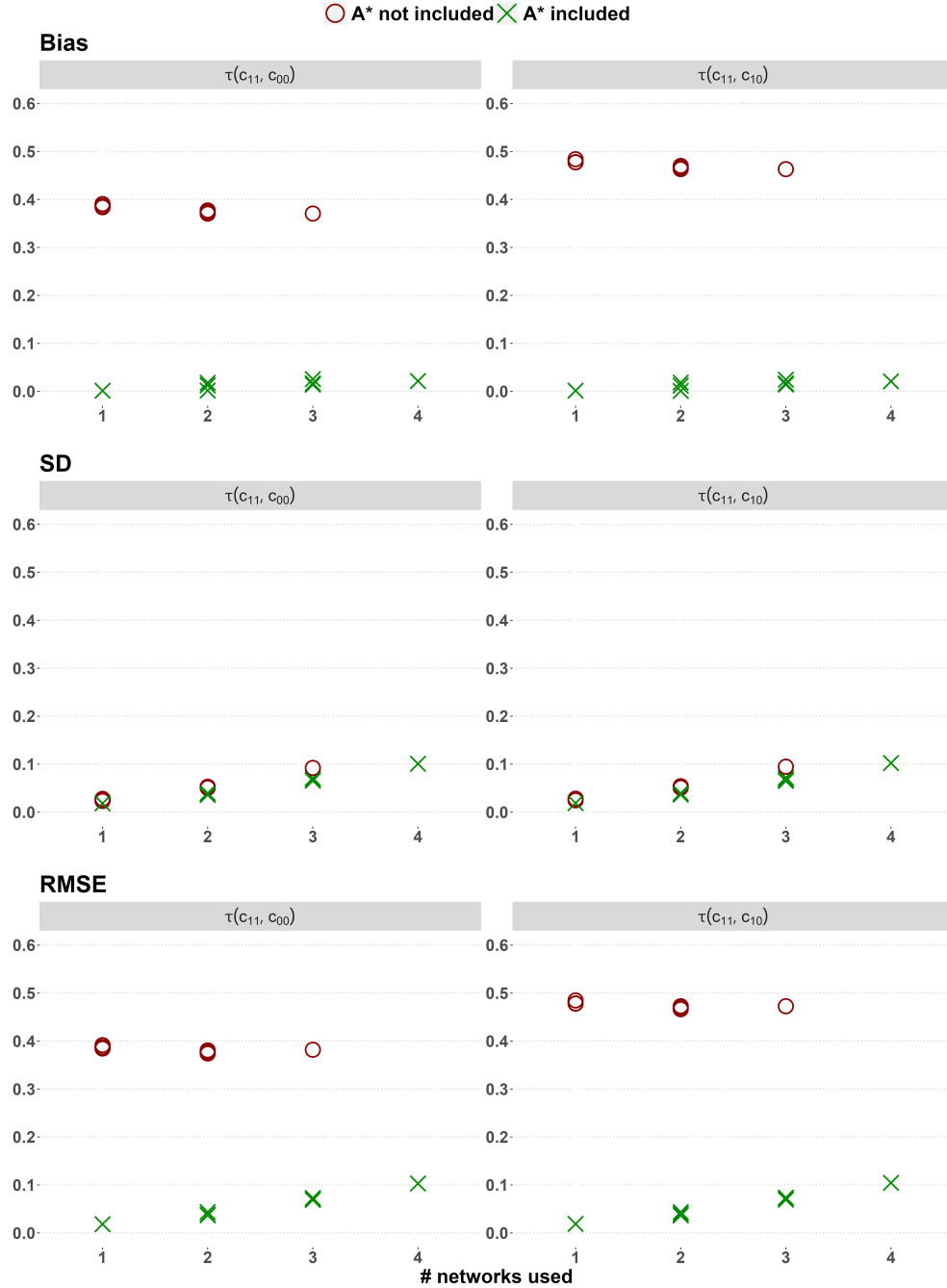


Figure F.11: Bias-variance tradeoff of the NMR estimator with \mathcal{A} being the four networks from Paluck et al. (2016) study. The results presented are the absolute bias, SD, and RMSE estimates of the Hajek NMR estimator. True causal effects are $\tau(c_{11}, c_{00}) = 1$ and $\tau(c_{11}, c_{10}) = 0.5$.

F.1.3 Conservative variance estimators

We illustrate the conservative property of the NMR variance estimators proposed in Appendix C in a small simulation study. In the same setup of the NMR bias-variance tradeoff simulation, we took all scenarios in which \mathcal{A} contained the true networks \mathbf{A}^* and compared the estimated conservative SE to the empirical SD. Figure F.12 displays the mean SE/SD

ratio of the overall effect $\tau(c_{11}, c_{00})$ across the 1000 iterations performed. Since all mean values are above one, we can surmise that the conservativeness property of the variance estimator holds. Nevertheless, it seems like the variance estimator is more conservative for Hajek than HT NMR estimators.

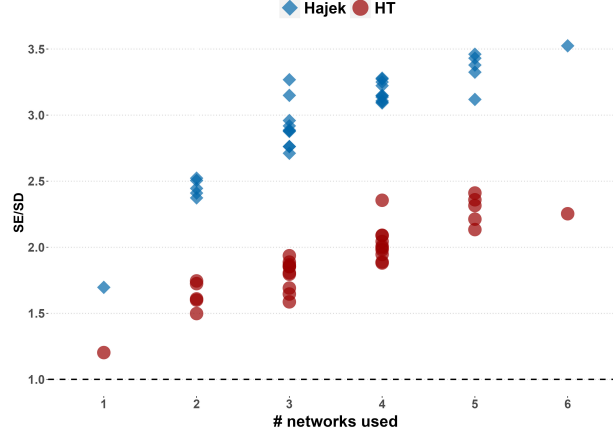


Figure F.12: Conservative NMR variance estimator. Values are the mean of $\tau(c_{01}, c_{00})$ estimated SE/SD.

F.2 Data analyses

F.2.1 Social network field experiment

In our analysis of the data, we performed the same data pre-processing conducted by Paluck et al. (2016). The open-source replicability package provided by Paluck et al. (2016) can be found at <https://www.icpsr.umich.edu/web/ICPSR/studies/37070>. Table F.5 is an extended version of the results displayed in the main text. It contains the estimation of two more estimands ($\tau(c_{011}, c_{000})$, $\tau(c_{111}, c_{000})$) using more networks combinations. For example, we also use the NMR with both the ST networks (measured at the two time periods) simultaneously.

| Networks | $\tau(c_{001}, c_{000})$ | | $\tau(c_{011}, c_{000})$ | | $\tau(c_{101}, c_{000})$ | | $\tau(c_{111}, c_{000})$ | |
|------------------|--------------------------|---------------|--------------------------|---------------|--------------------------|---------------|--------------------------|---------------|
| | HT | Hajek | HT | Hajek | HT | Hajek | HT | Hajek |
| ST-pre | 0.061 (0.217) | 0.146 (0.164) | 0.162 (0.353) | 0.122 (0.274) | 0.096 (0.272) | 0.271 (0.19) | 0.369 (0.53) | 0.272 (0.377) |
| BF-pre | 0.084 (0.254) | 0.123 (0.195) | 0.068 (0.349) | 0.162 (0.243) | 0.169 (0.361) | 0.265 (0.254) | 0.143 (0.504) | 0.292 (0.323) |
| ST-pre & BF-pre | 0.051 (0.198) | 0.134 (0.151) | 0.11 (0.449) | 0.135 (0.321) | 0.079 (0.247) | 0.261 (0.175) | 0.224 (0.627) | 0.258 (0.419) |
| ST-post | 0.06 (0.214) | 0.131 (0.164) | 0.137 (0.38) | 0.13 (0.282) | 0.116 (0.298) | 0.252 (0.212) | 0.251 (0.513) | 0.246 (0.355) |
| BF-post | 0.09 (0.262) | 0.135 (0.2) | 0.039 (0.268) | 0.09 (0.194) | 0.17 (0.362) | 0.258 (0.256) | 0.134 (0.497) | 0.297 (0.317) |
| ST-pre & ST-post | 0.037 (0.17) | 0.139 (0.13) | 0.231 (0.483) | 0.133 (0.37) | 0.071 (0.233) | 0.296 (0.161) | 0.469 (0.662) | 0.25 (0.493) |
| BF-pre & BF-post | 0.077 (0.244) | 0.124 (0.187) | 0.037 (0.271) | 0.063 (0.2) | 0.15 (0.339) | 0.258 (0.24) | 0.154 (0.549) | 0.303 (0.35) |
| ALL | 0.04 (0.177) | 0.178 (0.131) | 0.067 (0.397) | 0.051 (0.29) | 0.046 (0.19) | 0.227 (0.137) | 0.266 (0.802) | 0.226 (0.528) |

Table F.5: Extended results of the social network field experiment analysis. Results are reported as point estimates (SE). Estimation is performed using the NMR HT and Hajek estimators.

Table F.6 shows the Jaccard index of the four available networks. Clearly, networks derived from the same questions are more similar than those from different questions, e.g.,

the similarity of ST and ST-2 is 27.5% whereas those of ST and BF is 21.1%.

| | ST-pre | ST-post | BF-pre | BF-post |
|---------|--------|---------|--------|---------|
| ST-pre | 1 | | | |
| ST-post | 0.274 | 1 | | |
| BF-pre | 0.211 | 0.137 | 1 | |
| BF-post | 0.137 | 0.200 | 0.244 | 1 |

Table F.6: Jaccard index of all the four available networks from Paluck et al. (2016).

F.2.2 Cluster-randomized trial

In the analysis of the data, we performed all the data pre-processing Venturo-Conerly et al. (2022) conducted. The data and all relevant information are available in the open-source replicability files provided by the authors <https://osf.io/6qtjc/>.

We further performed a PBA with point mass distributions $q(\theta) = \mathbb{I}\{\theta = \theta^\dagger\}$ for a grid $\theta^\dagger \in \{0.0005, 0.001, \dots, 0.005\}$. The network deviation distribution $q(\mathbf{A}^* | \mathbf{A}^{sp}, \theta)$ is assumed to follow Scenario (I), i.e., randomly add an edge between students from different classes in the same school with probability θ . Figure F.13 displays the distribution of Hajek estimates across 200 PBA iterations (per θ^\dagger value). The estimates account only for systematic error from cross-cluster contamination without the further incorporation of random error due to the treatment allocation. Figure F.13 illustrates that as θ increases, so does the uncertainty across the point estimate. Displaying PBA results on a grid of increasing θ values is therefore appealing in situations where θ is one-dimensional since it enables researchers to plot the progression of the impact of network deviation as a function of θ . That is in comparison to the results shown in the main text (Scenario (I) & Uniform) that approximately integrate the estimates across the θ grid shown here.

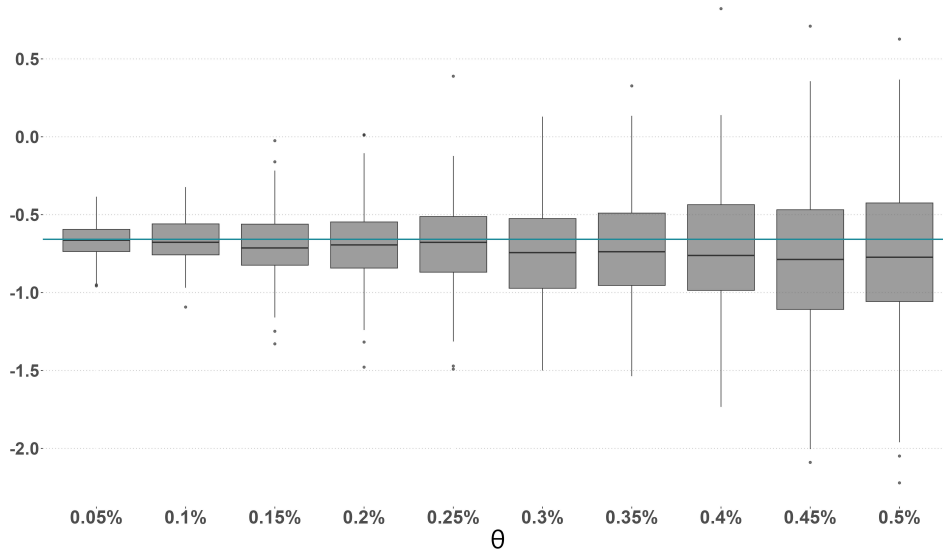


Figure F.13: PBA of CRT with point-mass distribution of θ . The horizontal cyan line at -0.658 is the point estimate under the no contamination baselines (see Section 7.2). Reported values are the Hajek estimates across 200 PBA iterations (per θ value) without the further incorporation of random error, i.e., the distribution of point estimates accounting for systematic error resulting from possible cross-cluster contamination.